AD-A148 765 USE OF P CODA FOR EXPLOSION MEDIUM AND IMPROVED YIELD 1/1
DETERMINATION(U) TELEDYNE GEOTECH ALEXANDRIA VA
ALEXANDRIA LABS I N GUPTA ET AL. 16 MAR 84
UNCLASSIFIED TGAL-TR-83-7A F08606-84-C-0009 F/G 18/3 NL

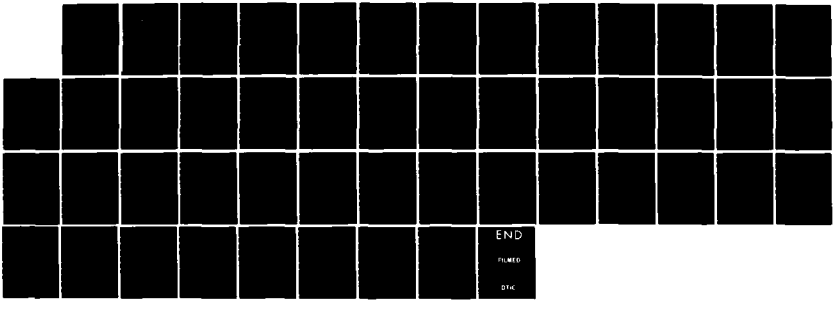

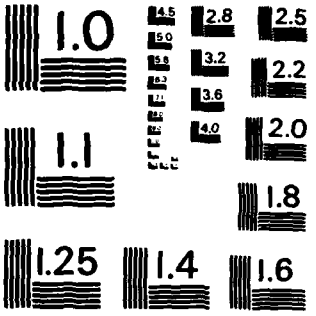

MICROCOPY RESOLUTION TEST CHART
NATIONAL BUREAU OF STANDARDS - 1963 - A

TGAL-TR-83-7a

USE OF P CODA FOR EXPLOSION MEDIUM AND IMPROVED YIELD DETERMINATION

I.N. Gupta, R.R. Blandford, R.A. Wagner, J.A. Burnetti and T.W. McElfresh

TELEDYNE GEOTECH
Alexandria Laboratories
314 Montgomery Street
Alexandria, VA 22314

16 March 1984

Technical Report

Prepared for:
DEFENSE ADVANCED RESEARCH PROJECTS AGENCY
1400 Wilson Boulevard
Arlington, VA 22209

Monitored by:
AFTAC/TG
Patrick Air Force Base
Florida 32925

Sponsored by

Defense Advanced Research Project Agency (DARPA)

ARPA Order No. 2551

Unclassified

SECURITY CLASSIFICATION OF THIS PAGE

REPORT DOCUMENTATION PAGE

1a. REPORT SECURITY CLASSIFICATION Unclassified	1b. RESTRICTIVE MARKINGS
2a. SECURITY CLASSIFICATION AUTHORITY	3. DISTRIBUTION/AVAILABILITY OF REPORT APPROVED FOR PUBLIC RELEASE; DISTRIBUTION UNLIMITED.
2b. DECLASSIFICATION/DOWNGRADING SCHEDULE	
4. PERFORMING ORGANIZATION REPORT NUMBER(S) TGAL-TR-83-7a	5. MONITORING ORGANIZATION REPORT NUMBER(S)
6a. NAME OF PERFORMING ORGANIZATION TELEDYNE GEOTECH Alexandria Laboratories 6b. OFFICE SYMBOL (If applicable)	7a. NAME OF MONITORING ORGANIZATION AFTAC/TG
6c. ADDRESS (City, State and ZIP Code) 314 Montgomery Street Alexandria, Virginia 22314	7b. ADDRESS (City, State and ZIP Code) Patrick Air Force Base Florida 32925
8a. NAME OF FUNDING/SPONSORING ORGANIZATION DARPA 8b. OFFICE SYMBOL (If applicable)	9. PROCUREMENT INSTRUMENT IDENTIFICATION NUMBER F08606-84-C-0009
8c. ADDRESS (City, State and ZIP Code) 1400 Wilson Boulevard Arlington, Virginia 22209	10. SOURCE OF FUNDING NOS. PROGRAM ELEMENT NO. / PROJECT NO. VT/4709 / TASK NO. 4.4 / WORK UNIT NO.
11. TITLE (Include Security Classification) (See Block 16)	
12. PERSONAL AUTHOR(S) I.N. Gupta, R. R. Blandford, R.A. Wagner, J.A. Burnetti and T.W. McElfresh	
13a. TYPE OF REPORT Technical 13b. TIME COVERED FROM Nov 82 TO Nov 83	14. DATE OF REPORT (Yr., Mo., Day) 84-03-16 15. PAGE COUNT 48
16. SUPPLEMENTARY NOTATION USE OF P CODA FOR EXPLOSION MEDIUM AND IMPROVED YIELD DETERMINATION	

17. COSATI CODES			18. SUBJECT TERMS (Continue on reverse if necessary and identify by block number)
FIELD	GROUP	SUB. GR.	P Coda, Yield, Explosion Medium, Magnitude
08	11	-	

19. ABSTRACT (Continue on reverse if necessary and identify by block number)

Spectral analyses of P and P coda on teleseismic recordings of nuclear explosions at Yucca Flats and Pahute Mesa regions of the Nevada Test Site (NTS) seem to provide explosion source medium information. The spectral ratio P/P-coda on short-period vertical component records at NORSAR shows positive correlation with explosion medium velocity. It seems that the initial P from generally shallower explosions within a low velocity medium experiences significantly lower scattering Q (and perhaps also inelastic Q) as compared to generally deeper explosions in a high velocity medium. Near-source scattering of explosion-generated Rayleigh waves into teleseismic P also appears to play an important role.

20. DISTRIBUTION/AVAILABILITY OF ABSTRACT UNCLASSIFIED/UNLIMITED ☒ SAME AS RPT ☐ DTIC USERS ☐	21. ABSTRACT SECURITY CLASSIFICATION Unclassified
22a. NAME OF RESPONSIBLE INDIVIDUAL Capt. Kenneth M. Ols	22b. TELEPHONE NUMBER (Include Area Code) 305-494-5263 22c. OFFICE SYMBOL TGR

DD FORM 1473, 83 APR EDITION OF 1 JAN 73 IS OBSOLETE

Unclassified

SECURITY CLASSIFICATION OF THIS PAGE

19. Continued

Magnitudes based on spectral integration of the initial P, when plotted against log yield, indicate considerable separation between the Yucca Flats and Pahute Mesa events whereas P coda shows no such evidence of source bias. Coda magnitudes provide significantly more precise measure of yield than the initial P. Moreover, after correcting the spectral displacement values for the effects of attenuation in the upper mantle and for source function spectrum based on knowledge of approximate yield or m_b, a plot of P-coda magnitude versus log yield appears to have a slope of unity. This implies that P coda from several stations (with different but known t* values) can be combined to further improve the yield determinations. Yields of several Soviet explosions are estimated on the basis of the NTS experience.

TABLE OF CONTENTS

	Page
LIST OF FIGURES	iv
LIST OF TABLES	vi
INTRODUCTION	1
COMPARISON OF P AND P CODA SPECTRA	3
VARIATIATION OF SPECTRAL RATIO P/P-CODA WITH EXPLOSION MEDIUM VELOCITY	14
P AND P CODA MAGNITUDES BASED ON SPECTRAL INTEGRATION	17
MAGNITUDES BASED ON SPECTRAL INTEGRATION FOR SOVIET EXPLOSIONS	26
DISCUSSION AND CONCLUSION	32
REFERENCES	33

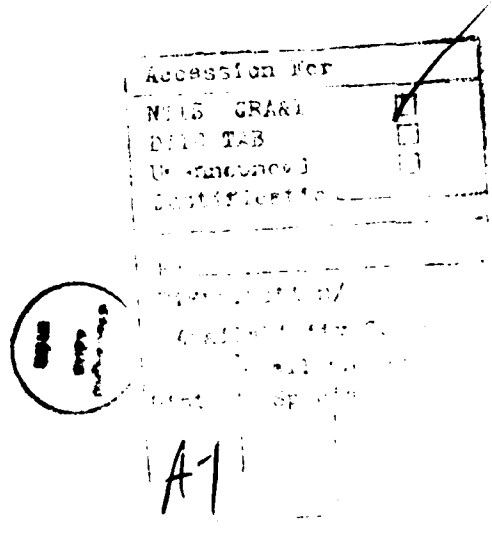

LIST OF FIGURES

Figure No.	Title	Page
1	NORSAR records of P and P coda from STRAIT and POOL showing time windows selected for initial P and P coda. Note that the energy in the initial P for the two explosions with nearly equal yields is considerably different whereas the P coda levels do not appear to be much different.	5
2a	Results from STRAIT recorded at NORSAR. Displacement spectra, not corrected for instrumental response, of the observed initial P signal (S) denoted by the symbol +, noise (N), symbol 0, for a window of equal length, and S-N, symbol *.	6
2b	Results from STRAIT recorded at NORSAR. Displacement spectra of P coda, similar to those in Figure 2a.	7
2c	Results from STRAIT recorded at NORSAR. Spectral ratio P/P-coda (corrected for noise), points for which the signal to noise power ratio is less than 2 are not plotted.	8
3a	Results from MAST recorded at NORSAR, similar to those for STRAIT in Figure 2a. Spectral nulls in initial P at about 1 and 2 Hz are distinct and can also be seen in the spectral ratio plot of Figure 3c.	10
3b	Results from MAST recorded at NORSAR, similar to those for STRAIT in Figure 2b.	11
3c	Results from MAST recorded at NORSAR, similar to those for STRAIT in Figure 2b.	12
4	Mean P/P-coda spectral slope for the frequency range 0.5 to 3.0 Hz versus average shot-point to surface or medium velocity for 14 explosions. The linear trend (dashed line) shows correlation coefficient of 0.896.	13
5	Spectral particle velocity (arbitrary units and integrated over the frequency range 0.5 to 3.0 Hz) plotted against log yield for the initial P from the fourteen NTS explosions. Lines of slope of 0.9 are drawn through data points for the four Yucca Flats events (upper line) and the ten Pahute Mesa events (lower line). For actual data points, see Appendix A.	18
6	Same as Figure 5 for P coda. A single line of slope 0.9 is drawn through data points for all fourteen events. For actual data points, see Appendix A.	19

LIST OF FIGURES (Continued)

Figure No.	Title	Page
7	Initial P integrated, spectral displacements with t* and granite source function corrections (arbitrary units) versus log yield for the fourteen NTS explosions. Lines of slope 1.0 are drawn separately for the four Yucca Flats events (upper line) and the ten Pahute Mesa events (lower line). If a single line of slope unity were drawn through all data points, the standard deviation of the intercept would be 0.14 magnitude unit. For actual data points, see Appendix A.	20
8	P coda integrated spectral displacement with t* and granite source function corrections (arbitrary units) plotted as a function of log yield. A line of slope 1.0 through all data points has an associated standard deviation of 0.06 magnitude unit. For actual data points, see Appendix A.	21
9	P coda integrated spectral displacement with t* and tuff source function corrections (arbitrary units) plotted versus log yield. A line of slope 1.0 through 13 data points (excluding the one with the smallest yield) gives a standard deviation of 0.07 magnitude unit. For actual data points, see Appendix A.	22
10	Similar to Figure 9 except that the tuff source function correction is based on approximate yields derived from m_b values. A line of slope 1.0 through the thirteen data points indicates a standard deviation of 0.09 magnitude unit. For actual data points, see Appendix A.	23
11	Initial P integrated spectral displacement with t* and granite source function corrections (arbitrary units) plotted as a function of m_b for 14 Soviet explosions. Mean slope is 0.75 ± 0.05 and the correlation coefficient is 0.97.	28
12	P coda integrated spectral displacement with t* and granite source function corrections (arbitrary units) versus m_b for 23 Soviet explosions. Mean slope is 0.70 ± 0.03 and the correlation coefficient is 0.98.	29
13	P coda spectral displacement (arbitrary units) plotted versus yield values obtained from Lg (Nuttli, 1983) on a log-log scale. The correlation coefficient is 0.82.	31

LIST OF TABLES

Table	Title	Page
1	NTS EXPLOSIONS USED IN STUDY	4
2	SHAGAN RIVER EXPLOSION USED IN STUDY	27

INTRODUCTION

Scattering of seismic waves due to departure from plane stratified media appears to play a vital role in the observed ground motion from nuclear explosions. A striking example is the transverse component Lg which is generally larger than the vertical or the radial component (Gupta and Blandford, 1983). Transverse Lg from explosions at the Nevada Test Site (NTS) has been found to be also a better estimator of yield than direct P (von Seggern and Alexander, 1984). At teleseismic distances, significantly greater stability of P coda (amplitudes and spectra) as compared to direct P has been pointed out and established in numerous recent studies (see, e.g. the review articles by Aki, 1982 and Bache, 1982). For a limited test area, P coda should therefore provide a more precise measurement of yield than the initial P. There are several mechanisms that may operate to make coda amplitudes more precise than the primary signal. P coda consists of scattered energy where most of the scattering takes place near the source and the receiver. Near-source scattering is perhaps mainly due to the scattering of source-generated surface waves to P body waves by topographic features and other impedance irregularities within several kilometers of the source (Greenfield, 1971). Contribution to teleseismic P from near-source scattering occurs for signals emerging over a large portion of the focal sphere so that the effects of reflection from the free surface (i.e., cancellation by pP) will be suppressed. Among others, Blandford and Shumway (1982) have remarked on the large variability of teleseismic P due to the effect of pP so that the use of coda may well remove this problem. The uniformity of coda amplitudes over the elements of an array for a single event suggests that coda is insensitive to the near-receiver focusing and defocusing effects that can drastically influence the primary arrival. This probably happens because (1) the energy scattered near the source and arriving directly at the receiver travels not along the path followed by the direct P but along numerous adjacent paths so that the coda may represent an average over the amplitudes generated within a relatively large source region; and (2) direct signals are received in a relatively large region surrounding the receiver and then scattered to the receiver, thus receiver focusing is averaged out.

Local or near-receiver scattering should influence initial P as well as the later arrivals. In fact, topography and other inhomogeneities near the receiver should, on the basis of reciprocity, be as significant scatterers as they are when near the source. Gupta and Blandford (1983) analyzed the spectral composition of the three orthogonal components of ground motion in the initial P waves from SALMON and concluded that local scattering is significant, especially at high frequencies. One may, however, expect near-source scattering to dominate over local scattering in some cases and local scattering to greatly exceed near-source scattering in certain other situations. In other words, only certain "clean" sites may be suitable for investigating near-source scattering. In this study, observations from the large aperture seismic array, NORSAR, located on Permian and older hard (mostly gneisses and granite) rocks are used. Large subsurface impedance contrasts should not exist at this locality so that near-receiver scattering should be low. Most of our analyses of P and P coda is carried out on records of explosions at NTS for which the yield and shot medium properties were known. Records of Soviet explosions at the Shagan site in the Semipalatinsk region are also examined and their yields estimated on the basis of the NTS experience.

COMPARISON OF P AND P CODA SPECTRA

Short-period, vertical component NORSAR records of fourteen (14) underground nuclear explosions (Table 1) were first selected for spectral analysis of initial P and the associated codas. The selection was made so as to observe the following criteria: (1) records of the center element of NORSAR subarray 01A, used in this study, were not clipped and had satisfactory signal to noise ratios; (2) accurate shot point to surface velocity (called medium velocity, hereafter) values, obtained by vibroseis or similar techniques, were available; events before 1970 could not therefore be used (Blandford et al., 1977); and (3) all events were below the water table and confined to Yucca Flats and Pahute Mesa regions of the NTS.

Figure 1 shows typical waveforms for the explosions STRAIT at Yucca Flats and POOL at Pahute Mesa. The yields of the two explosions are nearly equal. Both records have nearly the same peak amplitude values but the frequency contents of the initial P wavetrain appear to be quite different. The P codas on the two records, however, do not seem to be significantly different. The time windows used for spectral analyses of initial P and P coda, as indicated in Figure 1, are 12.8 sec and 25.6 sec long with the P window starting 4 sec before the onset of direct P. With digitization rate of 20 samples per second, the two windows, containing 256 and 512 points, respectively, were tapered with a Parzen window and Fourier transformed. The two spectra were smoothed over 4 and 8 points, respectively. The noise spectra were obtained in the same manner by using a time window immediately preceding the initial P window and of length 12.8 sec. The amplitude spectra of observed signal (S), noise (N) as well as S-N, uncorrected for instrumental response, for initial P and P coda from STRAIT, are shown in Figures 2a and 2b, respectively. The corresponding amplitude spectral ratio P/P-coda, corrected for noise by subtracting the power in noise from the power in observed signal, is shown in Figure 2c. For certain frequency values, the power in noise exceeded the power in the observed signal. Points for which S/N was less than 1.4 were not plotted on the P/P-coda plots. Similar spectra and spectral ratio P/P-coda for MAST are shown in

TABLE 1

NTS EXPLOSIONS USED IN STUDY

No.	Date	Name	Location	Medium	m_b(ISC)	Shot Depth	Medium Velocity*
1	28 Feb 1975	Topgallant	Yucca Flats	tuff	5.6	713.2m	1.653 km/sec
2	07 Mar 1975	Cabrillo	Yucca Flats	alluvium	5.4	600.5m	1.700 km/sec
3	14 May 1975	Tybo	Pahute Mesa	tuff	5.9	765.0m	2.275 km/sec
4	03 Jun 1975	Stilton	Pahute Mesa	rhyolite	5.8	731.5m	2.150 km/sec
5	19 Jun 1975	Mast	Pahute Mesa	rhyolite	5.9	911.3m	3.877 km/sec
6	28 Oct 1975	Kasseri	Pahute Mesa	tuff	6.2	1265.0m	3.040 km/sec
7	20 Nov 1975	Inlet	Pahute Mesa	rhyolite	5.9	819.0m	3.042 km/sec
8	20 Dec 1975	Chiberta	Yucca Flats	tuff	5.6	716.0m	1.840 km/sec
9	03 Jan 1976	Muenster	Pahute Mesa	tuff	6.2	1452.4m	2.900 km/sec
10	12 Feb 1976	Fontina	Pahute Mesa	tuff	6.1	1219.0m	2.860 km/sec
11	09 Mar 1976	Estuary	Pahute Mesa	rhyolite	5.8	868.1m	2.660 km/sec
12	14 Mar 1976	Colby	Pahute Mesa	tuff	6.2	1273.4m	2.790 km/sec
13	17 Mar 1976	Pool	Pahute Mesa	tuff	6.0	879.3m	2.865 km/sec
14	17 Mar 1976	Strait	Yucca Flats	tuff	5.8	780.3m	1.691 km/sec

* i.e. average P wave velocity from surface to shot point

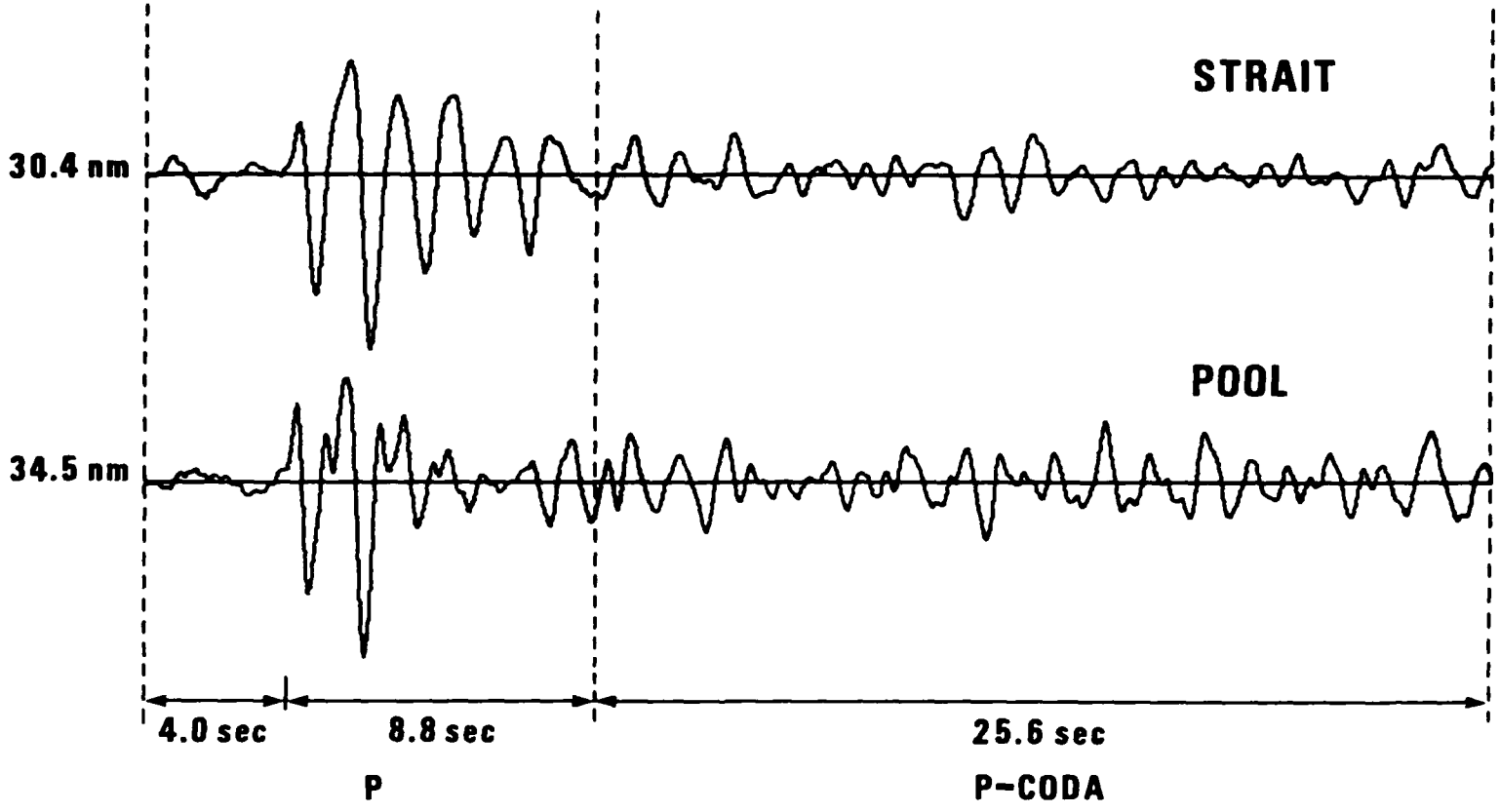

Figure 1 NORSAR records of P and P coda from STRAIT and POOL showing time windows selected for initial P and P coda. Note that the energy in the initial P for the two explosions with nearly equal yields is considerably different whereas the P coda levels do not appear to be much different.

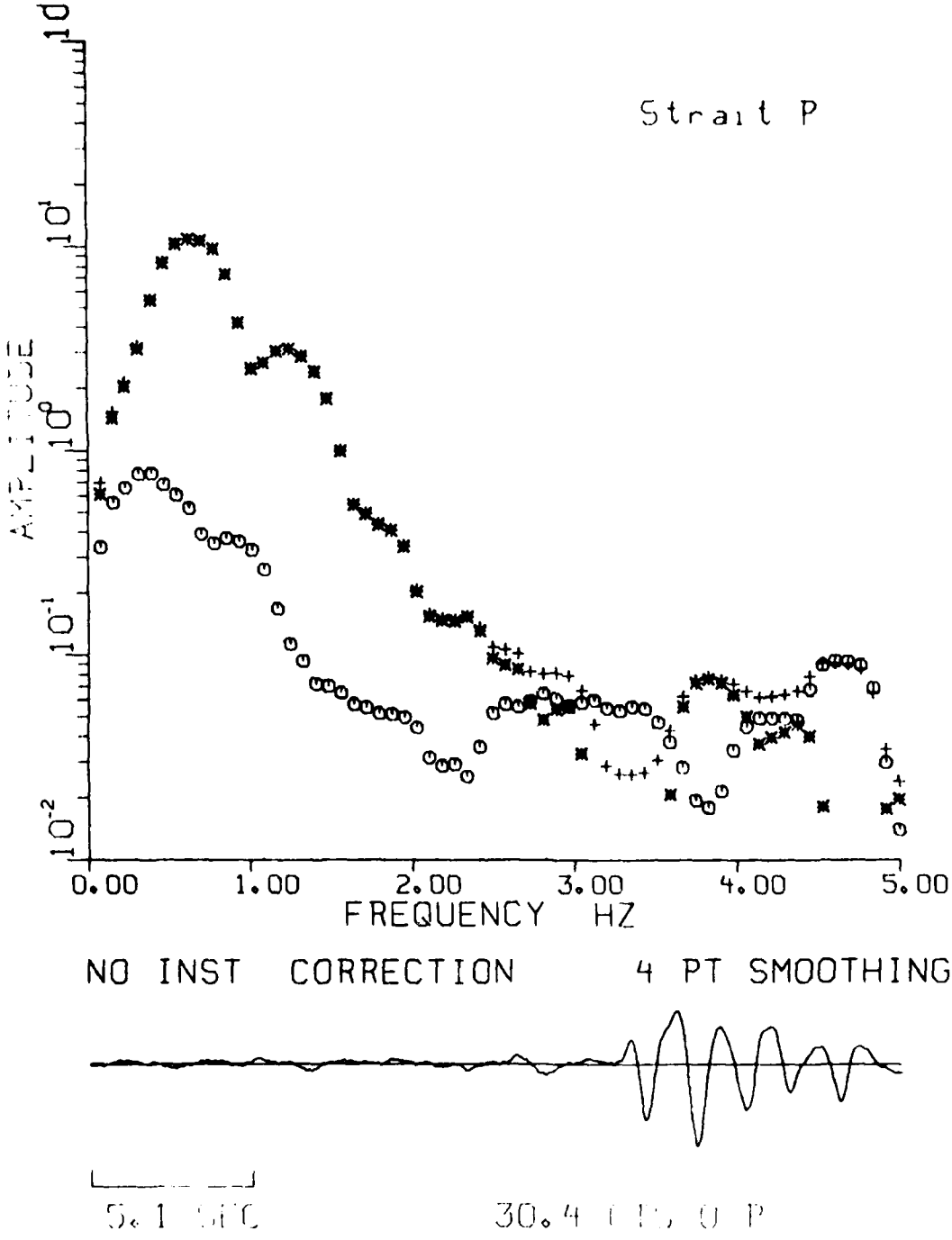

Figure 2a Results from STRAIT recorded at NORSAR. Displacement spectra, not corrected for instrumental response, of the observed initial P signal (S) denoted by the symbol +, noise (N), symbol 0, for a window of equal length, and S-N, symbol *.

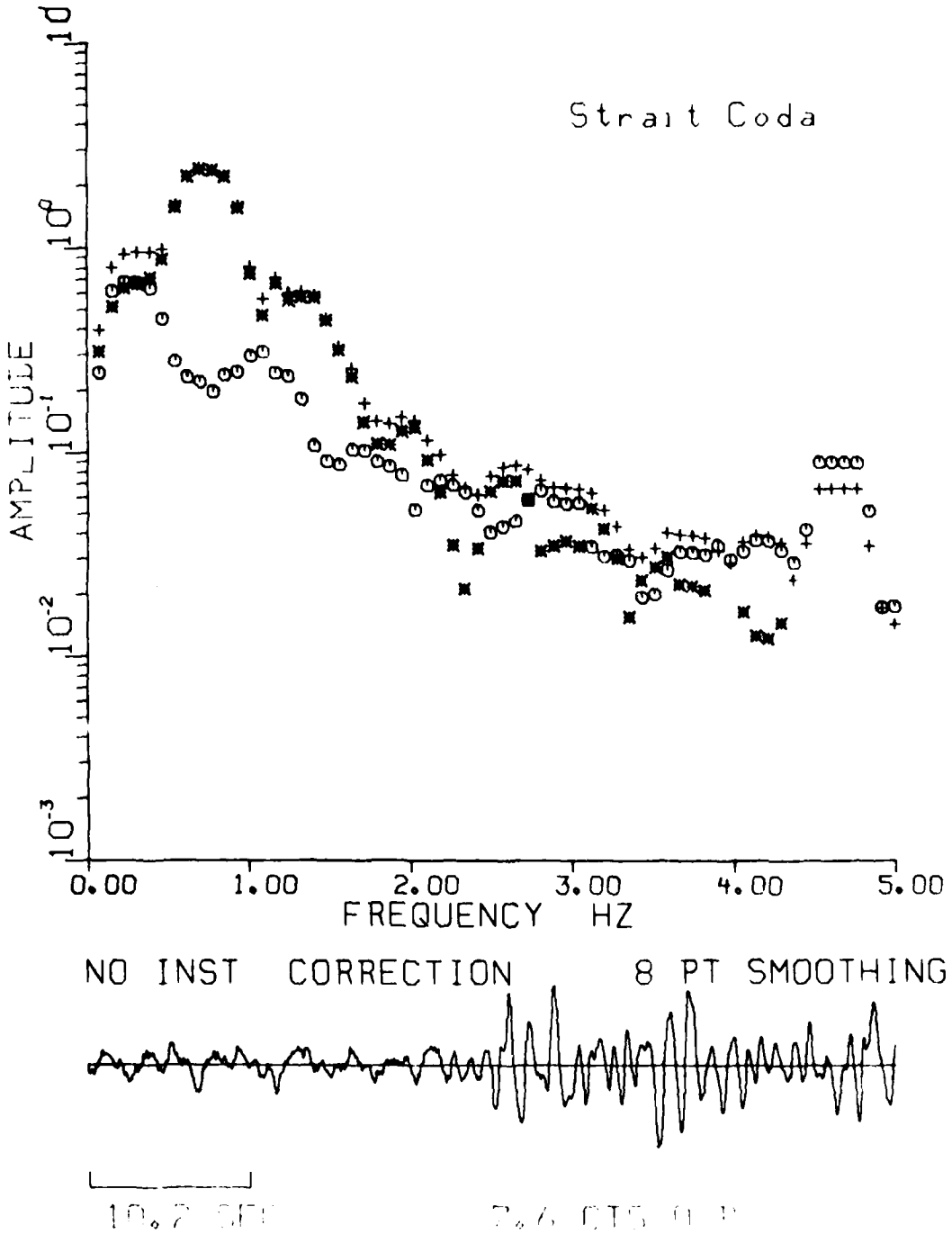

Figure 2b Results from STRAIT recorded at NORSAR. Displacement spectra of P coda, similar to those in Figure 2a.

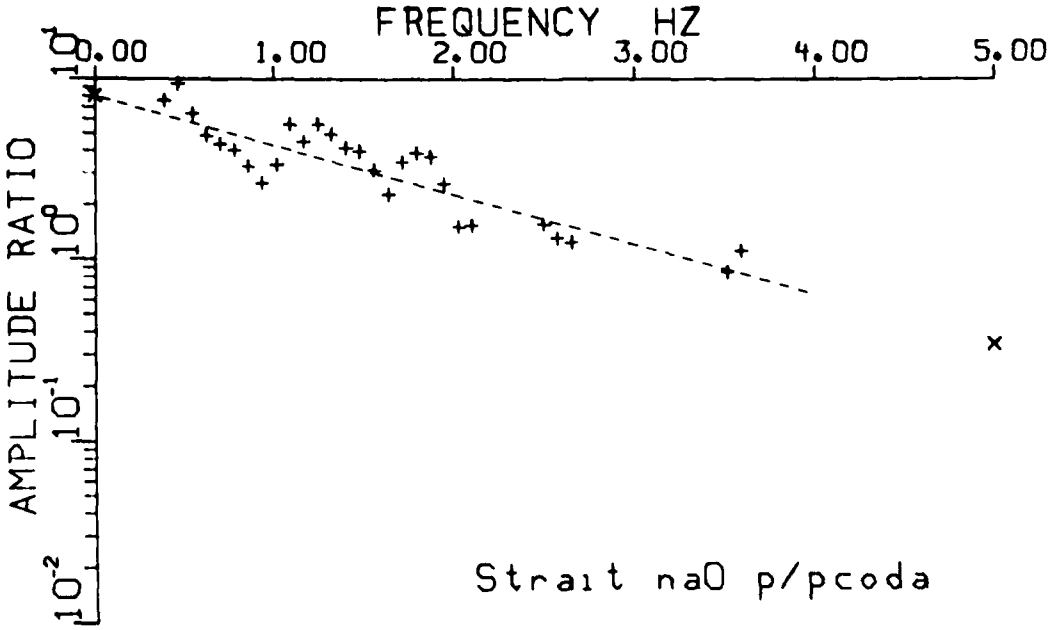

SLOPE = -0.2751 +/- 0.0409

Y INTERCEPT = 8.0993

0.5 - 3.0 HZ

Figure 2c **Results from STRAIT recorded at NORSAR. Spectral ratio P/P-coda (corrected for noise), points for which the signal to noise power ratio is less than 2 are not plotted.**

Figures 3a,b,c. For both explosions, S/N is good for frequencies up to about 3 Hz. The least squares mean slopes of the P/P-coda spectral ratios for the frequency range 0.5 to 3.0 Hz are indicated in Figures 2c and 3c.

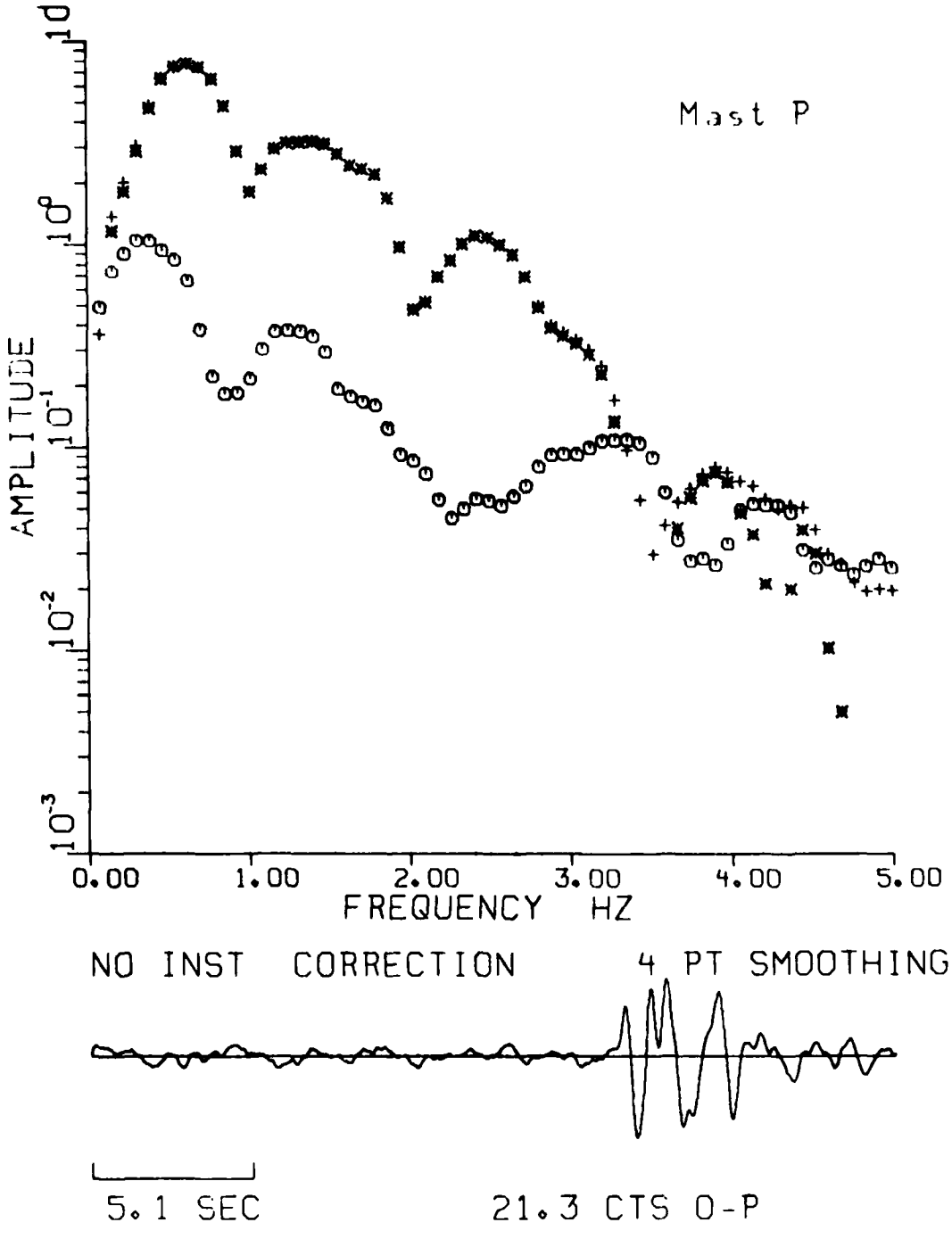

Figure 3a **Results from MAST recorded at NORSAR, similar to those for STRAIT in Figure 2a. Spectral nulls in initial P at about 1 and 2 Hz are distinct and can also be seen in the spectral ratio plot of Figure 3c.**

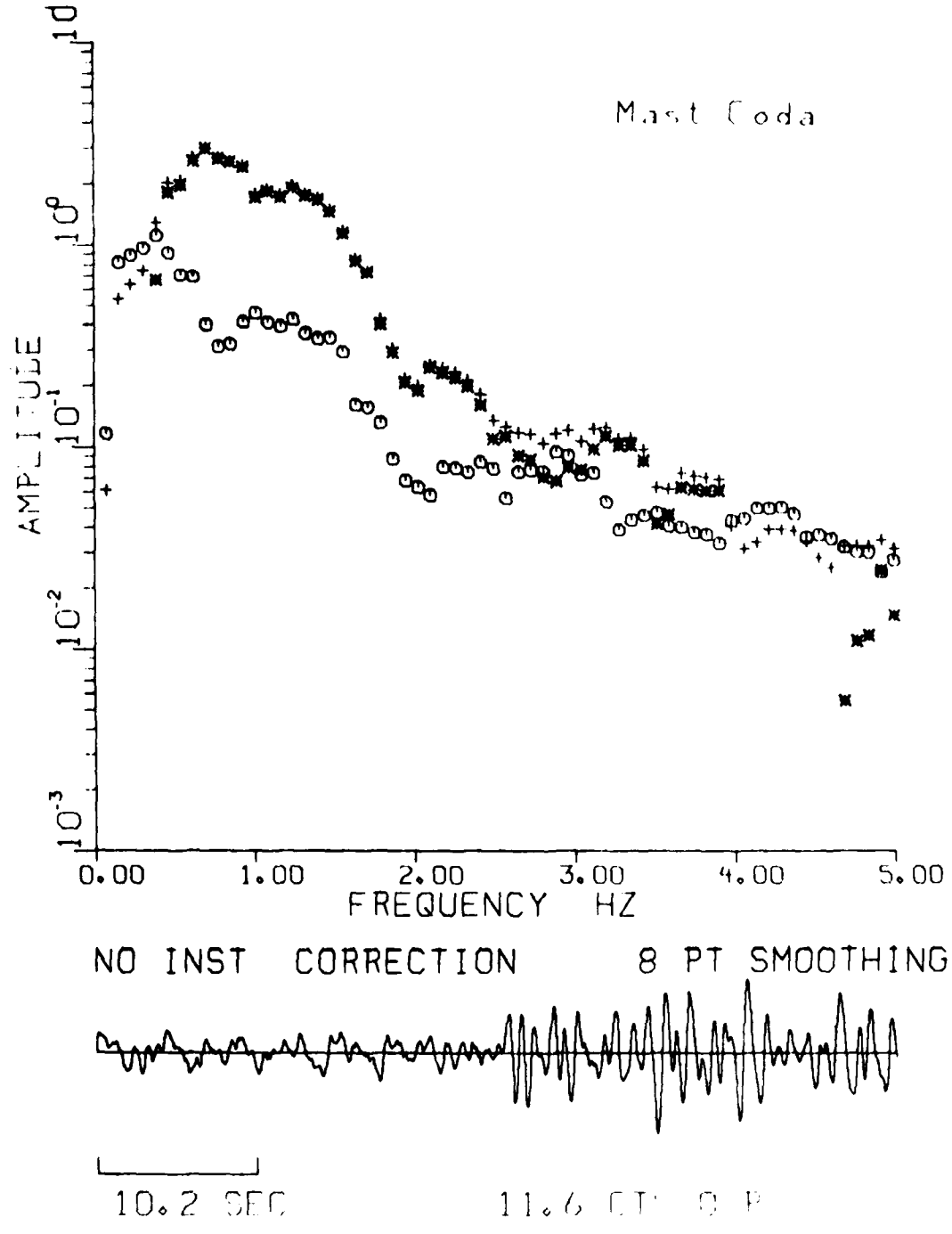

Figure 3b Results from MAST recorded at NORSAR, similar to those for STRAIT in Figure 2b.

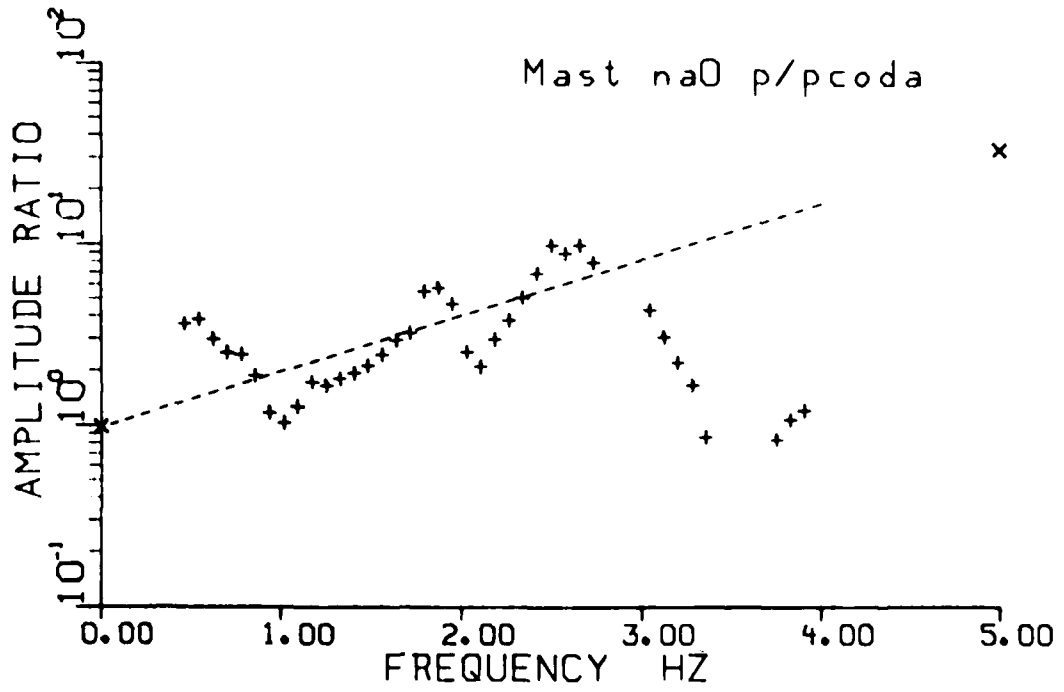

SLOPE = 0.3049 +/- 0.0530

Y INTERCEPT = 0.9849

0.5 - 3.0 HZ

Figure 3c Results from MAST recorded at NORSAR, similar to those for STRAIT in Figure 2b.

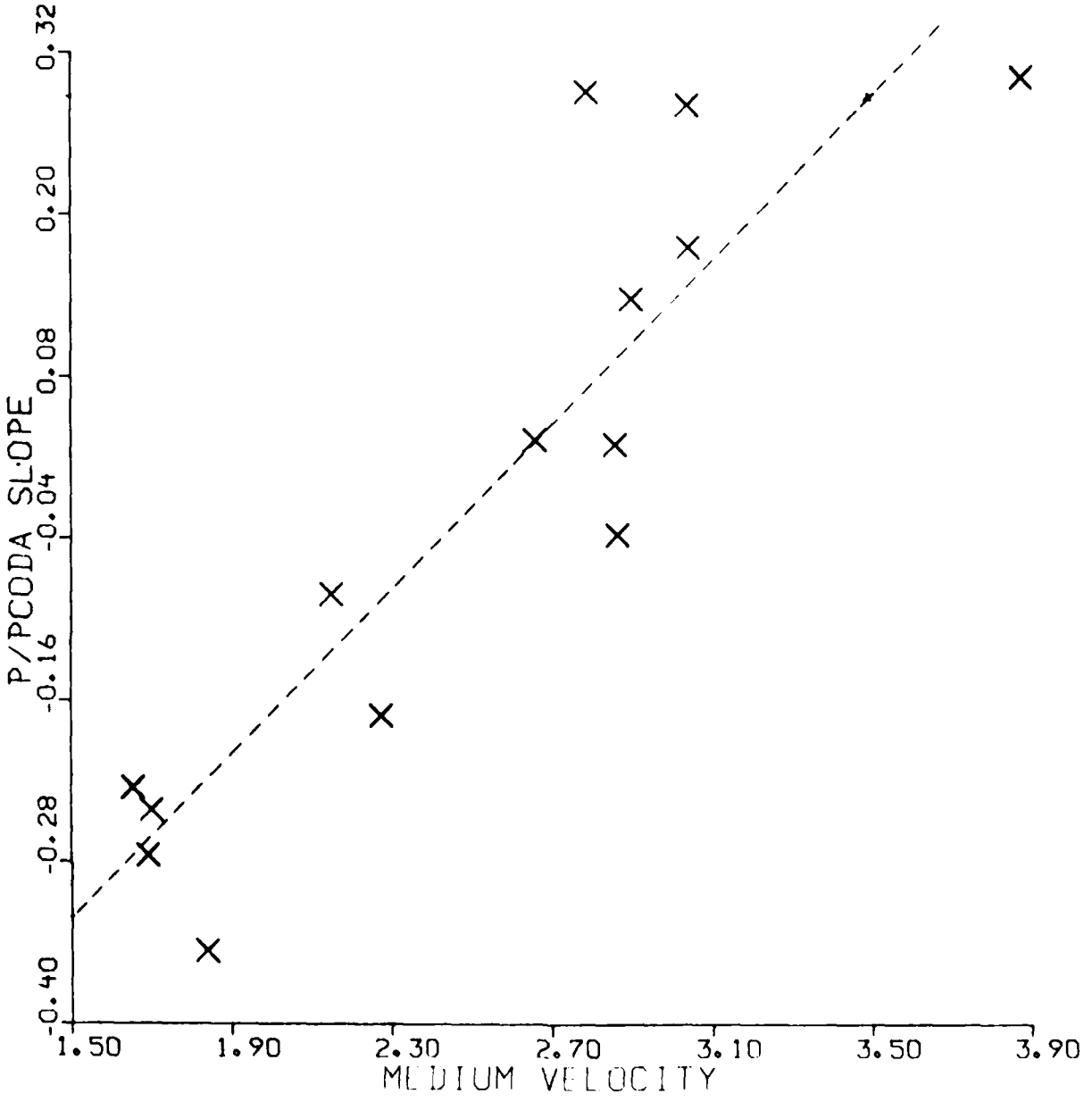

Figure 4 Mean P/P-coda spectral slope for the frequency range 0.5 to 3.0 Hz versus average shot-point to surface or medium velocity for 14 explosions. The linear trend (dashed line) shows correlation coefficient of 0.896.

VARIATION OF SPECTRAL RATIO P/P-CODA WITH EXPLOSION MEDIUM VELOCITY

A comparison of the spectra and spectral ratios in Figures 2 and 3 shows several interesting features. P coda spectra appear considerably smoother than the initial P spectra. The spectral holes observed in the P spectra due to cancellation by pP seem to have been filled in the P coda spectra. In fact, the spectral nulls for MAST have been estimated to be at about 1.0 Hz and 2.0 Hz (Shumway and Blandford, 1978). These are clearly seen on the spectra of Figure 3a but nearly absent in Figure 3b. These spectral nulls can also be seen on the spectral ratio in Figure 3c as spectral minima. For STRAIT, the spectral nulls (see Figure 2c) are not as well defined as for MAST. The spectral ratio P/P-coda, on the average, decreases with frequency for STRAIT and increases with frequency for MAST. In other words, initial P for STRAIT, an explosion in a low velocity medium (see Table 1) is richer in low frequencies compared to P coda whereas the opposite is true for MAST, an explosion in much higher velocity medium. The frequency dependence of spectral ratio P/P-coda appears to be related to the medium velocity and probably other properties of the near-field medium.

The spectral ratios P/P-coda were also obtained for 12 other explosions for which the explosion medium velocities were known. The least-squares mean slopes on P/P-coda plots (such as those in Figures 2c and 3c), are plotted against shot medium velocity in Figure 4 for all 14 explosions. There is considerable scatter among the data points but an approximately linear trend with correlation coefficient of 0.803 is obtained. The large variation in the ratios of P/P-coda for the 14 NTS explosions has to be mainly due to differences in the near-source region because the receiver is same and also because, for measurements at teleseismic distances, the effects of near-receiver structure would tend to be constant when the ratio of P to P-coda is taken.

Greenfield (1971) suggested that P coda from explosions is principally due to near-source scattering of short-period Rayleigh waves into P waves. The large amplitude explosion-generated Rayleigh waves slowly propagate outwards with appreciable energy for several tens of seconds and a fraction of this energy is gradually converted to P waves and radiated downwards to teleseismic distances.

A possible qualitative explanation for the dependence of the spectral ratio P/P-coda on the medium velocity can be offered by comparing shots in low and high velocity media. The initial P, as defined in Figure 1, consists mainly of direct P, pP and P waves derived from conversion of near-field Rayleigh waves (called R → P waves, hereafter). The observed stability of P coda and the variability of first P suggest the existence of small-scale heterogeneities in the earth's interior (Aki, 1982). In particular, from coherency measurements of near-field ground motion from an NTS explosion, McLaughlin et al. (1983) concluded that the upper 1 km or more of Pahute Mesa is heterogeneous at scale lengths less than 1 km. Scattering should therefore be greater for smaller wavelength or increase with frequency and decrease with the medium P-wave velocity. The region surrounding an explosion in a low velocity medium will act as a high scattering (low scattering Q) region not only because of the lower medium velocity but also because of generally greater impedance contrasts which increase the scattering efficiency. Furthermore, seismic energy from shots in low velocity media may enounter low inelastic Q near the source due to lower hydrostatic pressure (Stewart et al., 1983). All these factors make the initial P (comprising P, pP and R → P waves) from an explosion in low velocity medium deficient in high frequencies. Due to greater scattering, the high frequency energy is scattered away or removed from the initial P and some of it may appear later as P coda. This is similar to the apparent attenuation of a scattering medium described by Richards and Menke (1983). The initial P is therefore deficient in high frequencies as compared to P-coda. Note that the P coda used in this study, starting 8.8 sec after the first P and lasting for 25.6 sec (see Figure 1), is perhaps sufficiently delayed with respect to the first P so that its spectrum represents an average over such a large region around the shot point that the scattering effects of localized low or high velocity overburden lose their significance. The spectral ratio P/P-coda will therefore have a negative slope for explosions in low velocity medium. There will be much less scattering for explosions in high velocity medium so that the spectral ratio P/P-coda will have a smaller negative or even positive slope. This explanation is of course simplistic and purely qualitative because scattering is a complicated function not only of the medium velocity but also of numerous other parameters such as the actual size,

shape and location of the heterogeneities. Source depth and the presence of topographic features in the source region are also expected to play important roles. The former strongly influences the generation of short-period Rayleigh waves (Hudson and Douglas, 1975) whereas the latter may strongly control the conversion of surface waves to teleseismic P (Hudson et al., 1973). A detailed investigation using the finite difference technique on more realistic models of explosions in various media is planned for the future.

P AND P CODA MAGNITUDES BASED ON SPECTRAL INTEGRATION

Using P and P coda windows specified earlier, spectra corrected for noise and instrumental response were first obtained for the 14 explosions listed in Table 1. Particle velocities integrated over several frequency ranges such as 0.5 to 3.0 Hz, 0.5 to 2.0 Hz, and 1.0 to 3.0 Hz (referred to as spectral particle velocity) were obtained and plotted against the known yield of explosions on a log-log scale. The signal to noise ratio for most explosions fell off rapidly beyond 3 Hz so that frequencies higher than 3 Hz were not considered to be useful. The frequency range 0.5 to 3.0 Hz appeared to provide better correlation with yield than the other frequency ranges. The results for P and P coda are shown in Figures 5 and 6, respectively.* The data for P show large scatter and the Yucca Flats and Pahute Mesa events appear to separate out. For P coda, there is no clear distinction between the Yucca Flats and Pahute Mesa events. On the basis of commonly accepted explosion source time functions (e.g. von Seggern and Blandford, 1972), the spectrally integrated magnitude versus yield data should show a mean slope of less than unity (see, for example, Blandford, 1976). An attempt is made to fit a slope of 0.9 to the data in Figures 5 and 6.

The integrated spectral magnitudes are subject to variations similar to those for time domain measurements. The effect of pP, which has a modulating effect on the spectra, will in general be somewhat smoothed out as compared to its time domain counterpart. P coda should be nearly free from the effects of pP. The effect of attenuation due to the upper mantle structure is also important (Blandford, 1976; Marshall et al., 1979) and should equally apply to P and P coda. A correction for the effects of attenuation was therefore applied to the spectral

---

* These two figures (as well as Figures 7,8,9 and 10) do not show the actual data points because the yield values are classified. Complete figures are available in Appendix A (classified).

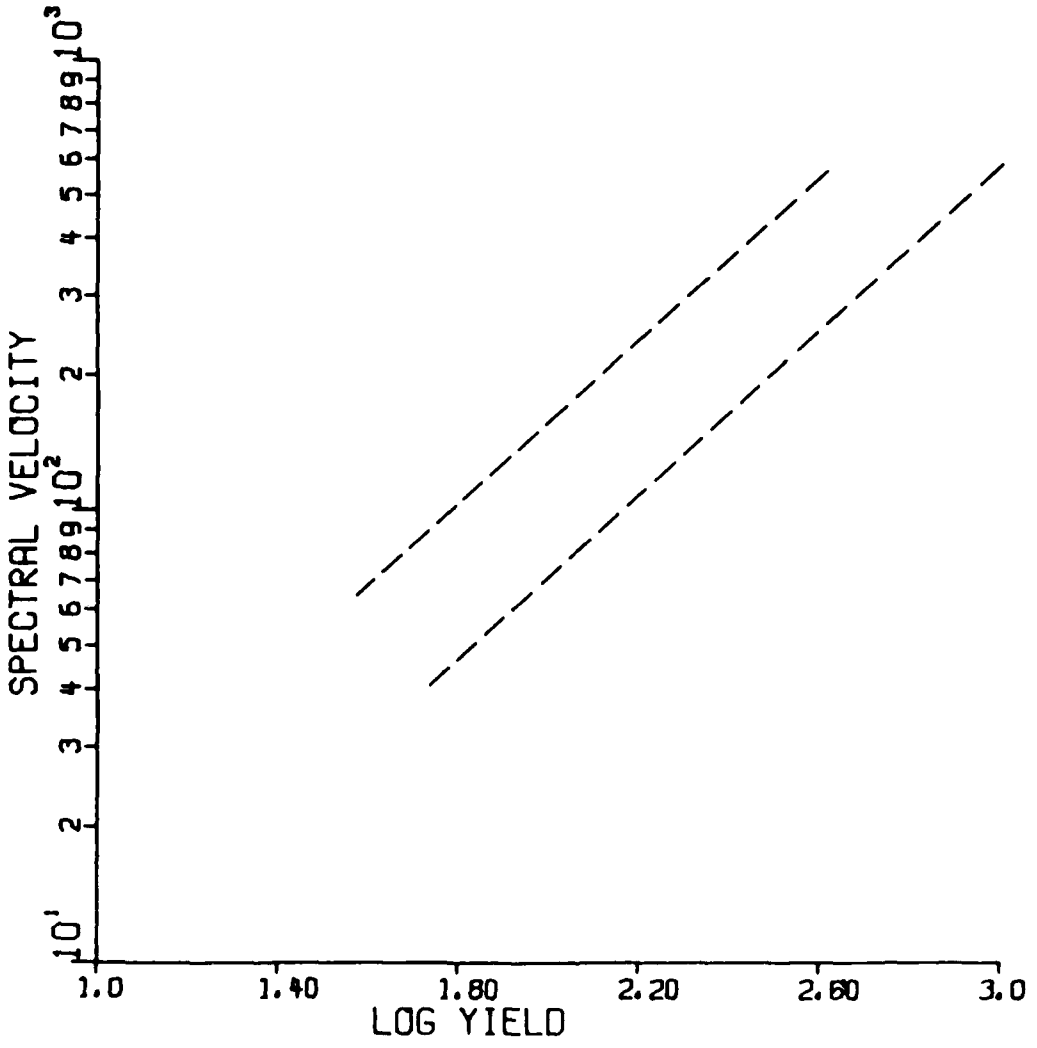

Figure 5 Spectral particle velocity (arbitrary units and integrated over the frequency range 0.5 to 3.0 Hz) plotted against log yield for the initial P from the fourteen NTS explosions. Lines of slope of 0.9 are drawn through data points for the four Yucca Flats events (upper line) and the ten Pahute Mesa events (lower line). For actual data points, see Appendix A.

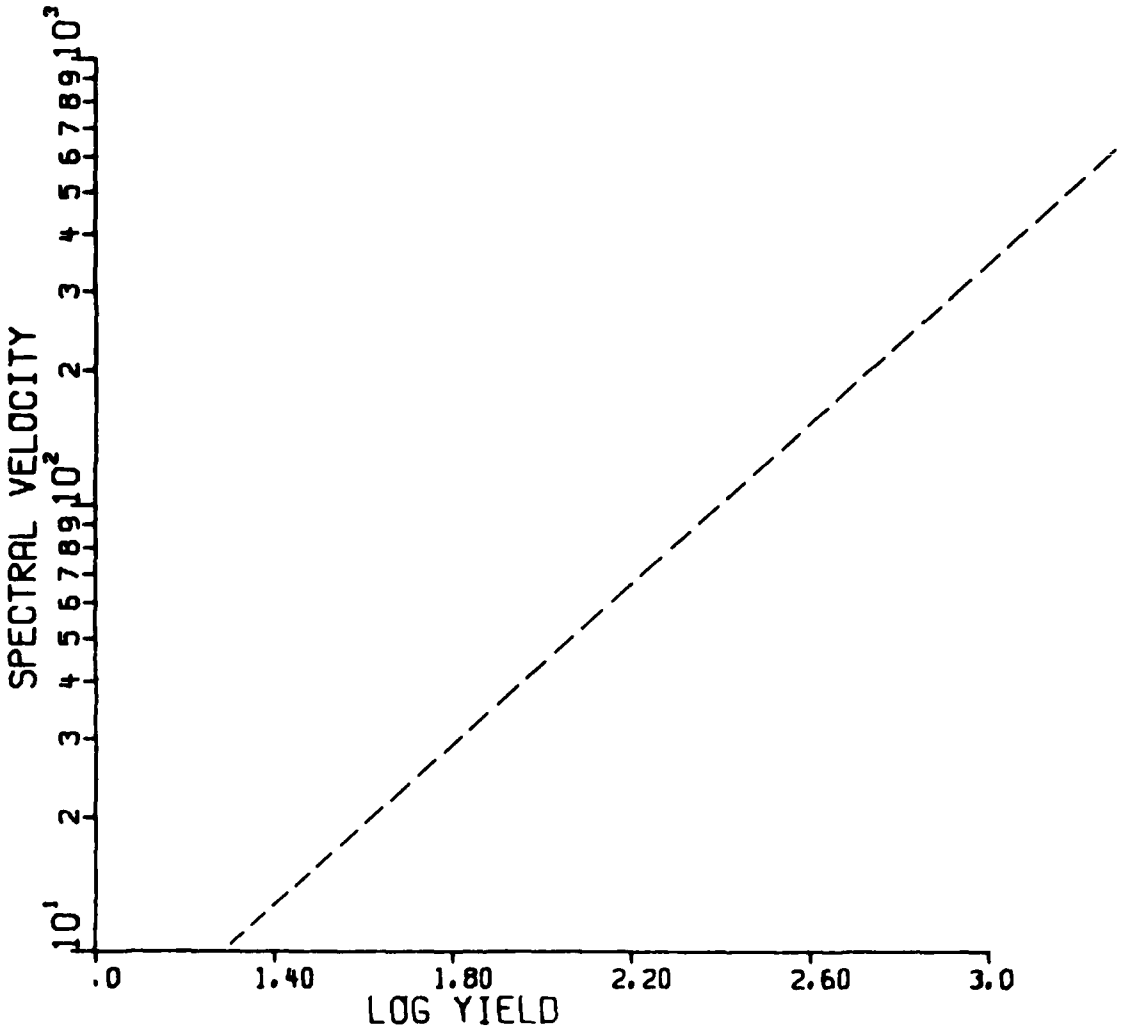

Figure 6 Same as Figure 5 for P coda. A single line of slope 0.9 is drawn through data points for all fourteen events. For actual data points, see Appendix A.

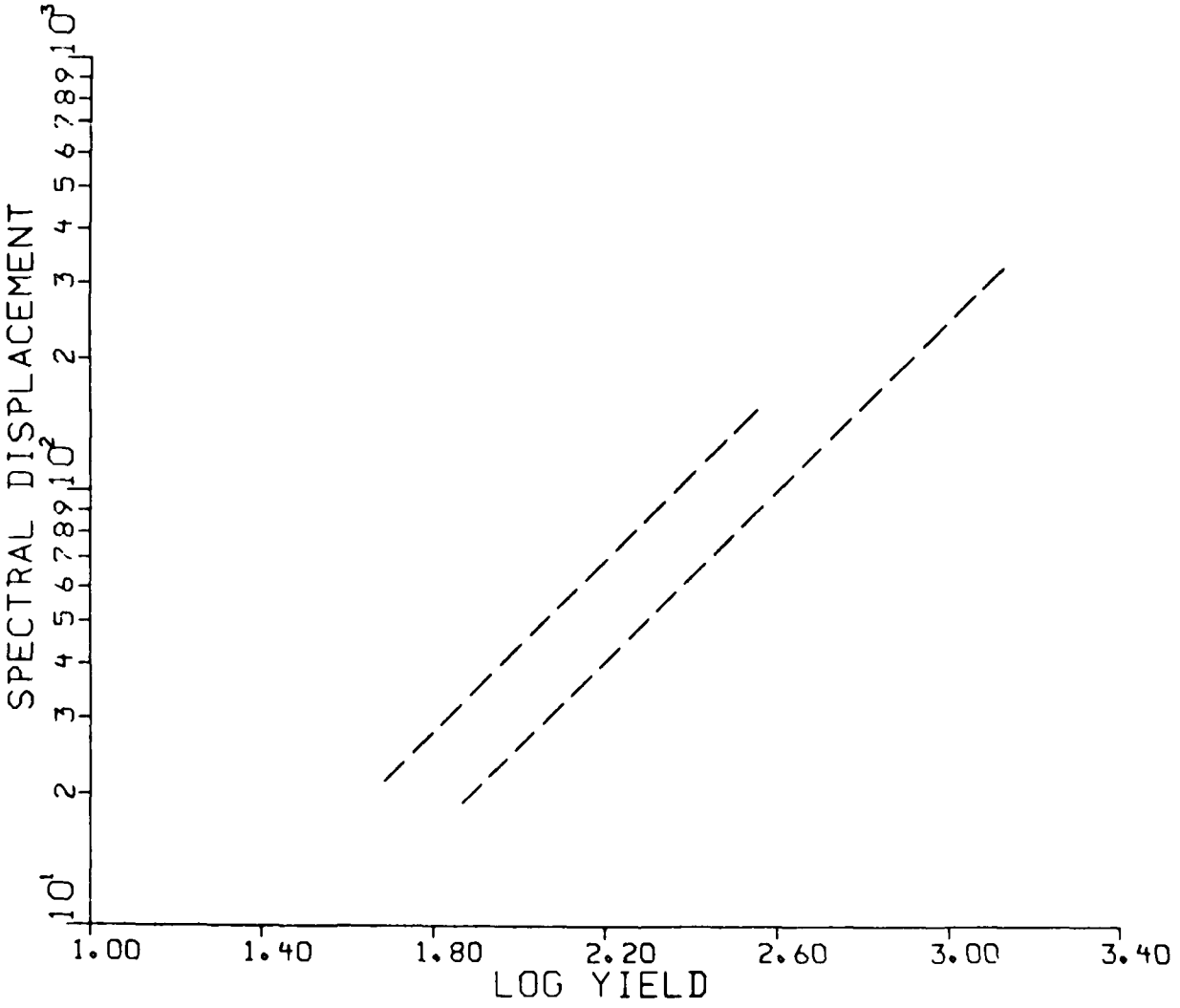

Figure 7 Initial P integrated, spectral displacements with t* and granite source function corrections (arbitrary units) versus log yield for the fourteen NTS explosions. Lines of slope 1.0 are drawn separately for the four Yucca Flats events (upper line) and the ten Pahute Mesa events (lower line). If a single line of slope unity were drawn through all data points, the standard deviation of the intercept would be 0.14 magnitude unit. For actual data points, see Appendix A.

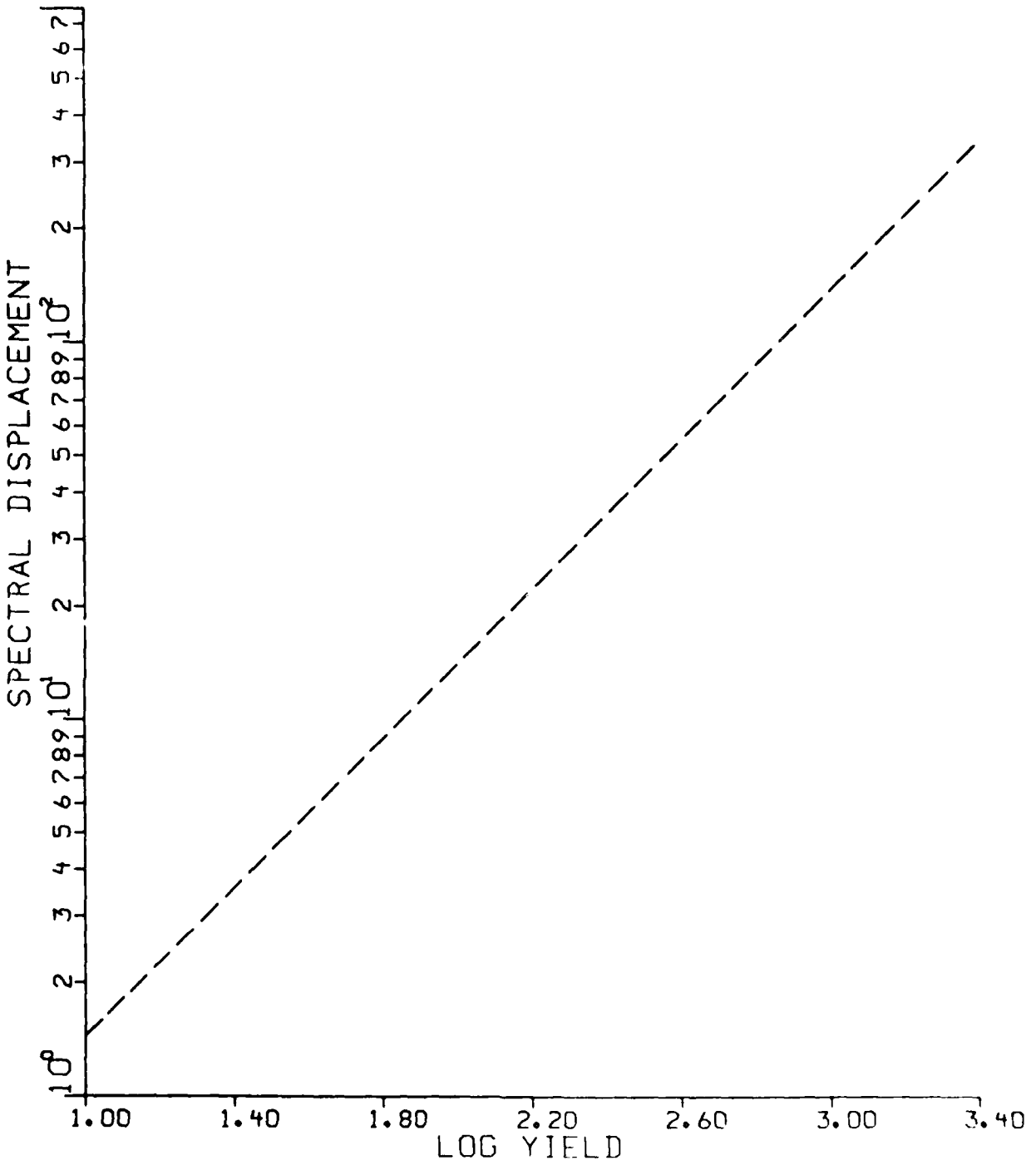

Figure 8 P coda integrated spectral displacement with t* and granite source function corrections (arbitrary units) plotted as a function of log yield. A line of slope 1.0 through all data points has an associated standard deviation of 0.06 magnitude unit. For actual data points, see Appendix A.

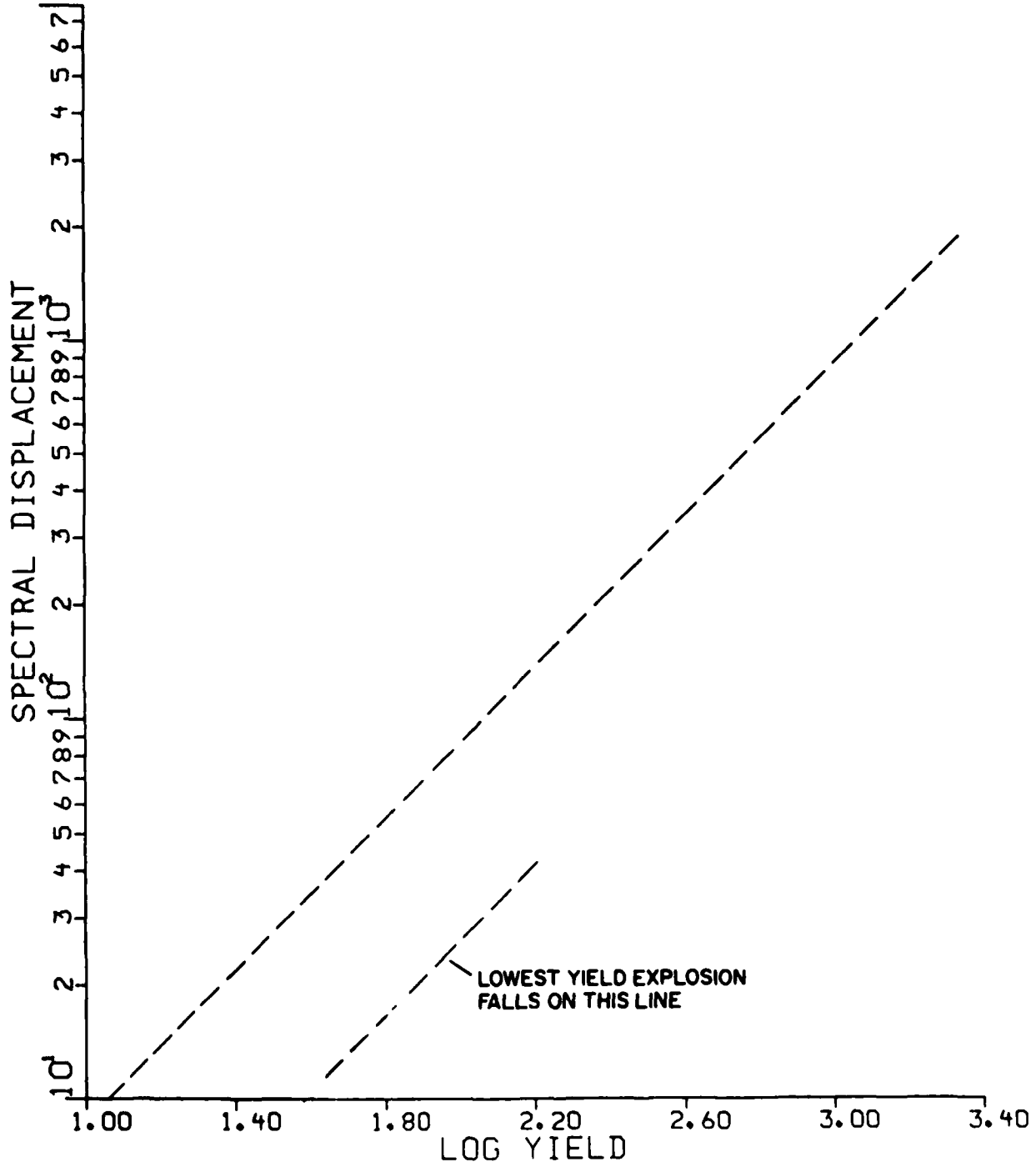

Figure 9 P coda integrated spectral displacement with t* and tuff source function corrections (arbitrary units) plotted versus log yield. A line of slope 1.0 through 13 data points (excluding the one with the smallest yield) gives a standard deviation of 0.07 magnitude unit. For actual data points, see Appendix A.

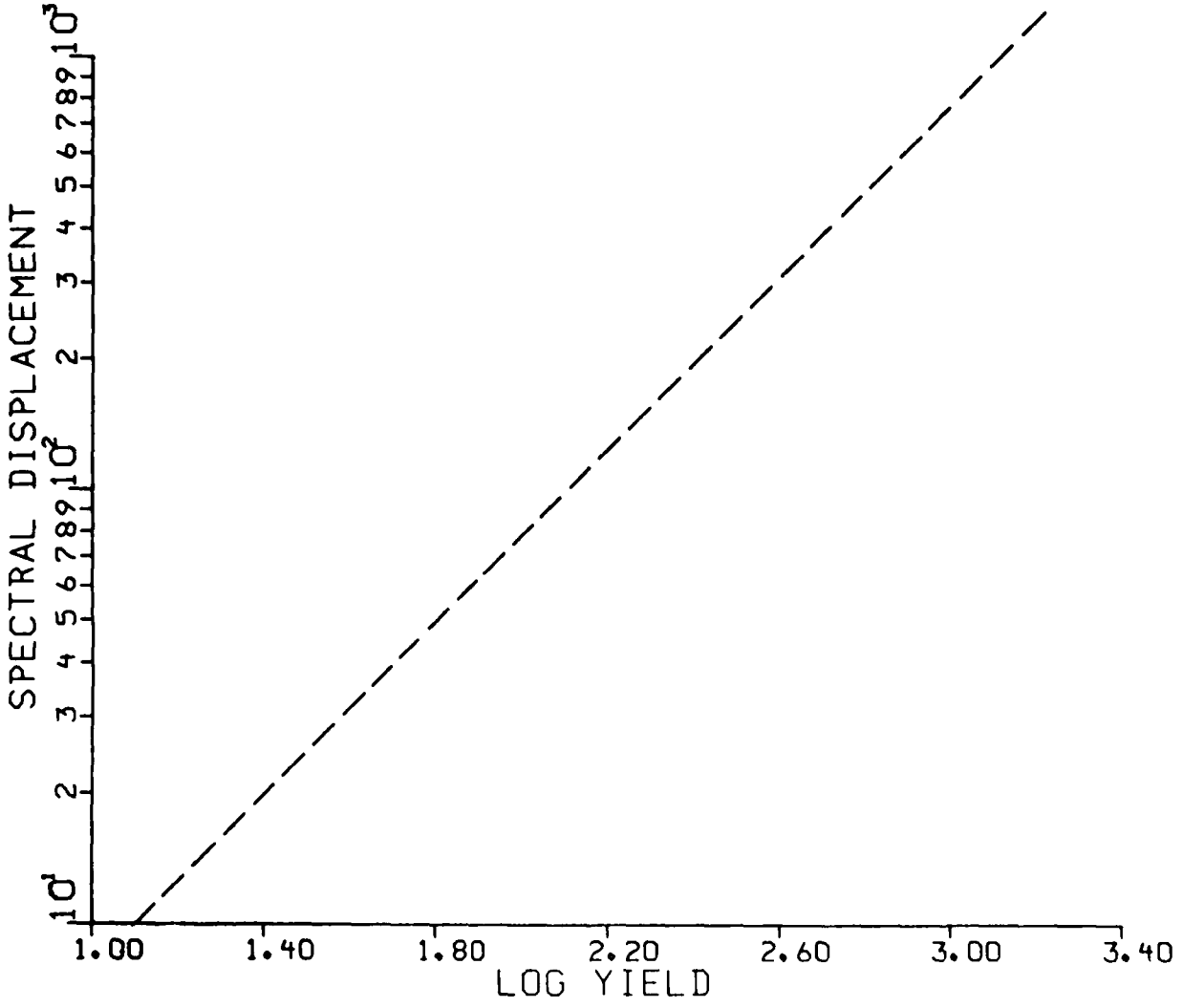

Figure 10 Similar to Figure 9 except that the tuff source function correction is based on approximate yields derived from m_b values. A line of slope 1.0 through the thirteen data points indicates a standard deviation of 0.09 magnitude unit. For actual data points, see Appendix A.

data by assuming $t^* = 0.4$, the value appropriate for NTS shots recorded at NORSAR (Der, et al., 1983). The particle displacement value for each frequency, f was therefore multiplied by the term exp (π f t^*). Finally, a correction for the source function was applied using the von Seggern and Blandford (1972) source time function for the known yields of the 14 NTS explosions. The source function for a given yield, Y may be expressed as

$$S(\omega) = Y \frac{[A^2(\frac{\omega}{k})^2 + 1]^{1/2}}{[(\frac{\omega}{k})^2 + 1]^{3/2}} \psi(\infty) \qquad (1)$$

where $\omega = 2\pi f$, $\psi(\infty)$ is a coupling term independent of frequency, and

$$k = k_o (5/Y)^{1/3} \qquad (2)$$

where A and k_o are medium-dependent constants. The source function correction is therefore the multiplication of the particle displacement values by $S(o)/S(\omega)$. With these two corrections, the integrated spectral magnitude versus yield plots should ideally have a slope of unity.

The 14 NTS explosions used in this study were mostly in tuff and rhyolite (only one was in alluvium, see Table 1). All shots were below the water table so that, following Blandford (1976), we used the granite reduced displacement potential (RDP) for teleseismic P (i.e. A = 5.08 and $k_o = 16.8$). For P coda, we first tried the same granite RDP. P coda is, however, derived mainly from waves propagating upwards and sideways so that, again following Blandford's (1976) suggestion, a source function for tuff (A = 1.0, $k_o = 12.0$) was also attempted. The results for P and P coda, with both t^* and source function corrections, are given in Figures 7, 8 and 9.

Comparing the two sets of results, spectral integration of initial P in Figure 7 is similar to that in Figure 5 but with somewhat smaller source bias between the Yucca Flats and Pahute Mesa events. Considering all 14 explosions, the standard deviation, σ, associated with fitting a slope of 1 is 0.14 magnitude unit (m.u.). A comparison of the results for P coda in Figures 8 and 6 appears to show some improvement when t^* and source function corrections are applied. Moreover, a slope of unity

seems to be valid for the data in Figures 8 and 7. Obtaining a slope of unity has practical significance since it suggests that corrections for source function and t^* can appropriately be applied to P coda so that results from several stations (each with its own t^* value) can be properly combined to further improve the yield determinations. The standard deviation for the P coda data in Figure 8 is only 0.06 m.u. The corresponding P coda results based on the source function for tuff (Figure 9) indicate σ of 0.07 m.u., if the smallest yield explosion is excluded. The latter seems to be an outlier perhaps because of reasons such as its being the only explosion in alluvium, only 34m below the water table and its record at NORSAR having low signal to noise ratio. In any case, the results for P coda (Figures 8 and 9) have significantly less scatter than initial P, with $\sigma \sim 0.07$ m.u. Note that this low value of σ is nearly the same as for yield estimates from regional Lg waves for NTS explosions when results from several stations were combined (Nuttli, 1983).

In a real situation, one would like to use the P coda from an explosion to estimate its yield so that the value of yield necessary for applying the source function correction will not be available. We therefore needed to test how good the P coda estimates can be if only approximate yields such as those from known m_b values are known. For NTS tuff/rhyolite events, Bache (1982) suggested the following relationship between magnitude, $\overline{m}_2$ (see Marshall et al., 1979) and yield, Y

$$\overline{m}_2 = 3.71 + 0.89 \log Y \qquad (3)$$

with $\sigma = 0.09$. One may assume m_2 to be the same as m_b(ISC). Knowing the m_b value for the 13 tuff/rhyolite explosions in Table 1, we obtained their approximate yields from equation (3) and applied the corresponding source function correction based on the tuff RDP. The results are shown in Figure 10 in which the integrated spectral displacement is plotted against the log of actual yield. Assuming a slope of unity, the standard deviation, σ is 0.09 m.u., only slightly greater than the earlier value of 0.07 m.u. Note that several yield values derived from the use of equation (3) differ from the actual (classified) yields by nearly a factor of 2. Comparing Figures 9 and 10, it seems that source function correction based on approximate yields works almost as well as when based on actual yields.

MAGNITUDES BASED ON SPECTRAL INTEGRATION FOR SOVIET EXPLOSIONS

Twenty three explosions from the Shagan River region of the Eastern Kazakh test area of the USSR, with satisfactory recordings at NORSAR were selected (Table 2). P and P coda magnitudes were obtained using the same procedure as for the NTS explosions but the frequency range was increased to 0.5 to 5.0 Hz since nearly all records showed good signal to noise ratios for frequencies up to at least 5 Hz. The correction for attenuation in the upper mantle for Shagan explosions recorded at NORSAR requires $t^* = 0.15$ (Der et al., 1983). Since the yield of the Soviet explosions is not known, the source function correction could not be applied in the same maner as for the NTS explosions. An alternative approach, described below, was therefore used to obtain approximate values of yield which were then used to apply the source function corrections.

Using an improved general linear model technique on a large amount of short-period data, Blandford et al. (1983) deduced that a yield of 150 kton for a Shagan explosion should correspond to m_b of 6.17. Marshall et al. (1979) defined a new magnitude, m_Q which correlates well with yield for explosions at various test sites. The explosions at Shagan are believed to be in hard rock similar to granite so that their empirical relationship for explosions in salt and granite

$$m_Q = 4.26 + 1.00 \log Y \qquad (4)$$

(see Figure 6b, Marshall et al., 1979) should be applicable. One may also write

$$m_Q = m_b(\mathrm{ISC}) + C \qquad (5)$$

where C is a constant. From equations (4) and (5)

$$\log Y = m_b(\mathrm{ISC}) + C - 4.26 \qquad (6)$$

Using the information that for Y = 150 kton, $m_b(\mathrm{ISC}) = 6.17$, equation (6) gives $C = 0.27$ so that

$$\log Y = m_b(\mathrm{ISC}) - 3.99 \qquad (7)$$

Knowing m_b(ISC) for the Shagan explosions (Table 2), the yield can thus be estimated and the source function correction can be applied. A granite RDP was assumed. Results for P and P coda are shown in Figures 11 and 12, respectively, where m_b(ISC) is plotted against the spectral displacement. There are only 14 data points for P since P was clipped for 9 explosions; P coda was however available for all events. The results for initial P (Figure 11) show a mean slope of 0.75 $\pm$ 0.05

TABLE 2

SHAGAN RIVER EXPLOSIONS USED IN STUDY

No.	Date	Location (ISC)	m_b(ISC)	Yield from Nuttli (1983)
1	02 Nov 1972	49.91N, 78.85E	6.1	170
2	23 Jul 1973	49.94N, 78.85E	6.1	229
3	31 May 1974	49.91N, 78.91E	5.9	62
4	16 Oct 1974	49.99N, 78.96E	5.5	20
5	27 Dec 1974	49.91N, 79.05E	5.6	63
6	27 Apr 1975	49.94N, 79.02E	5.6	35
7	29 Oct 1975	49.92N, 78.91E	5.8	33
8	25 Dec 1975	50.02N, 78.86E	5.7	93
9	21 Apr 1976	49.89N, 78.83E	5.3	17
10	09 Jun 1976	49.98N, 79.07E	5.3	21
11	04 Jul 1976	49.85N, 78.97E	5.8	112
12	28 Aug 1976	49.95N, 78.98E	5.8	49
13	29 May 1977	49.86N, 78.84E	5.8	47
14	29 Jun 1977	49.96N, 78.91E	5.3	16
15	05 Sep 1977	50.05N, 78.93E	5.8	39
16	11 Jun 1978	49.88N, 78.81E	5.9	74
17	05 Jul 1978	49.84N, 78.91E	5.8	59
18	15 Sep 1978	49.91N, 78.94E	6.0	105
19	04 Nov 1978	50.03N, 78.98E	5.6	46
20	23 Jun 1979	49.89N, 78.92E	6.2	120
21	07 Jul 1979	50.05N, 79.06E	5.8	105
22	04 Aug 1979	49.86N, 78.94E	6.1	157
23	14 Sep 1980	49.94N, 78.86E	6.2	200

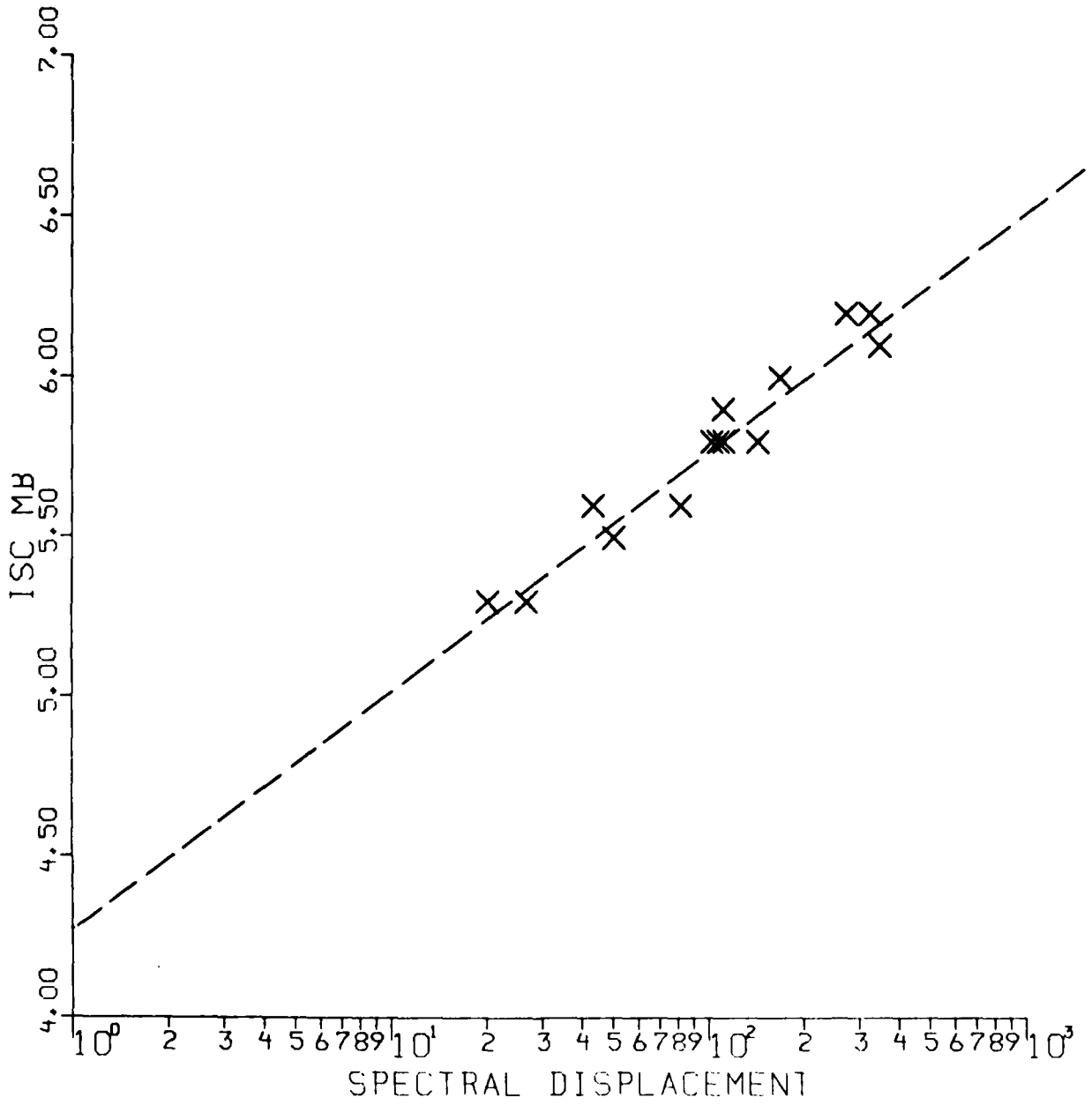

Figure 11 **Initial P integrated spectral displacement with t* and granite source function corrections (arbitrary units) plotted as a function of m_b for 14 Soviet explosions. Mean slope is 0.75 $\pm$ 0.05 and the correlation coefficient is 0.97.**

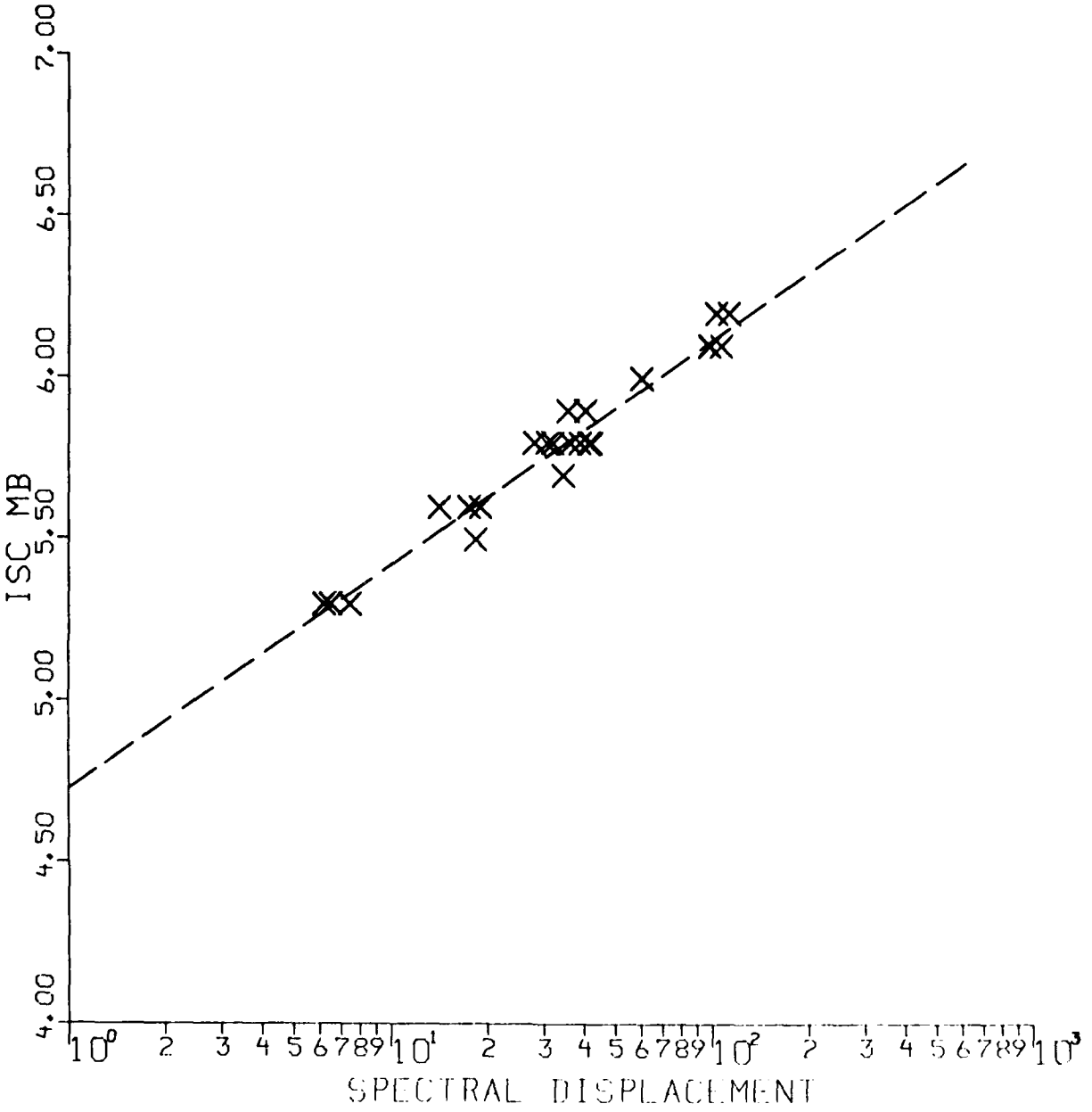

Figure 12 P coda integrated spectral displacement with t* and granite source function corrections (arbitrary units) versus m_b for 23 Soviet explosions. Mean slope is 0.70 $\pm$ 0.03 and the correlation coefficient is 0.98.

(i.e. standard deviation of 0.05) and correlation coefficient of 0.97. The standard deviation of magnitude estimate, σ is 0.07. For P coda (Figure 12), mean slope is 0.70 $\pm$ 0.03, correlations coefficient is 0.98 and σ = 0.06. As one would expect, correlation with m_b is better for P coda than for P. There is of course no way of checking how well the spectral displacement values correlate with actual yields. It is, however, interesting to note that the observed slope of about 0.7 for both P and P coda agrees well with the slope derived for magnitude-yield curves on the basis of the source function for granite and t^* = 0.15 (see Figure 7, Blandford, 1976).

Using short-period Lg waves recorded at regional distances at a number of stations, Nuttli (1983) estimated the yield of all the Soviet explosions used in this study; these values are also listed in Table 2. A plot of these yield values versus coda spectral displacement values (Figure 13) shows rather poor correlation (correlation coefficient of 0.91). In other words, our coda displacement values do not correlate well with Nuttli's yield values. It is, however, found that the AFTAC classified m_b values correlate better with our coda displacement values (correlation coefficient = 0.97) than with Nuttli's yield values (correlation coefficient = 0.94). This perhaps means that yields based on P coda at a single station are at least as accurate as those derived from Lg recorded at a number of stations.

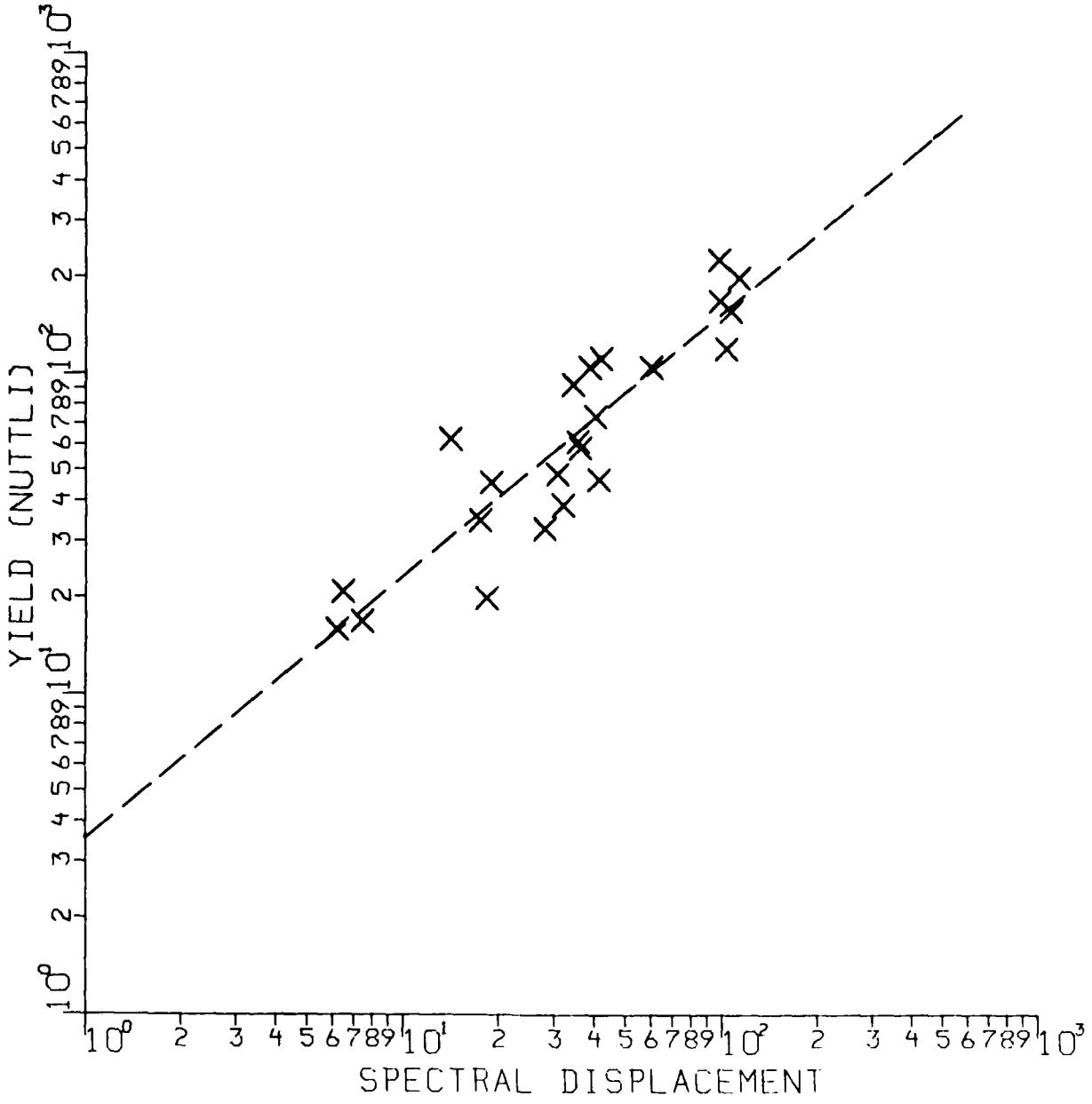

Figure 13 **P coda spectral displacement (arbitrary units) plotted versus yield values obtained from Lg (Nuttli, 1983) on a log-log scale. The correlation coefficient is 0.82.**

DISCUSSION AND CONCLUSION

Our results from spectral analyses of P and P coda of NTS explosions offer the exciting possibility of obtaining source medium information from short-period teleseismic data. The positive correlation between the spectral ratio P/P-coda and explosion medium velocity is encouraging. Other factors such as depth of burial, subsurface velocity and density distribution, topography are also bound to influence the spectra of P and its coda so that more sophisticated analyses incorporating these factors should lead to considerably more information about the explosion source and its environment.

Magnitudes based on spectral integration of P coda from NTS explosions provide a much more reliable measure of yield than the initial P. Furthermore, the spectral displacement of P coda seems to be linearly related to yield after corrections for the effects of attenuation in the upper mantle and source function based on knowledge of approximate yield (or m_b) have been applied. Slope of 1 on spectral displacement versus yield plots (on a log-log scale) suggests that results from several stations can be combined to further improve the yield determinations. It is also hoped that information regarding the source medium, such as that derived from the spectral ratio P/P-coda, can also be used to further improve the yield estimates.

Spectral integration of P and P coda from Soviet explosions within the Shagan River region show m_b to correlate better with spectral displacements from P coda than those from the initial P. There is of course no way of verifying how well the coda values correlate with yield. It seems, however, that P coda from a single station can provide at least as good estimates of yield as those from Lg based on a network of stations.

REFERENCES

Aki, K. (1982). Scattering and attenuation, Bull. Seism. Soc. Am., 72, S319-S330.

Bache, T. (1982). Estimating the yield of underground nuclear explosions, Bull. Seism. Soc. Am., 72, S131-S168.

Blandford, R. R. (1976). Experimental determination of scaling laws for contained and cratering explosions, SDAC-TR-76-3, Teledyne Geotech, Alexandria, Virginia.

Blandford, R. R. and R. H. Shumway (1982). Magnitude-yield for nuclear explosions in granite at the Nevada Test Site and Algeria: joint determination with station effects and with data containing clipped and low-amplitude signals, VSC-TR-82-12, Teledyne Geotech, Alexandria, Virginia.

Blandford, R. R., R. H. Shumway and R. Wagner (1983). Magnitude yield for nuclear explosions at several test sites with allowance for station effects, truncated data, amplitude correlation between events within test sites, absorption, and pP, VSC-TR-83-15, Teledyne Geotech, Alexandria, Virginia.

Blandford, R. R., M. R. Tillman and D. P. Racine (1977). Empirical m_b:M_s relations at the Nevada Test Site with application to m_b-yield relations, SDAC-TR-76-14, Teledyne Geotech, Alexandria, Virginia.

Der, Z. A., T. W. McElfresh, R. Wagner and A. O'Donnell (1983). Global t* measurements for the magnitude yield experiment, SDAC-TR-82-3, Teledyne Geotech, Alexandria, Virginia.

Greenfield, R. J. (1971). Short-period P-wave generation by Rayleigh-wave scattering at Novaya Zemlya, J. Geophys. Res., 76, 7988-8002.

Gupta, I. N. and R. R. Blandford (1983). A mechanism for generation of short-period transverse motion from explosions, Bull. Seism. Soc. Am., 73, 571-592.

Hudson, J. A. and A. Douglas (1975). On the amplitudes of seismic waves, Geophys. J., 42, 1039-1044.

Hudson, J. A., R. F. Humphryes, I. M. Mason and V. K. Kembhavi (1973). The scattering of longitudinal elastic waves at a rough free surface, J. Phys. D: Appl. Phys., 6, 2174-2186.

Marshall, P. D., D. L. Springer and H. C. Rodean (1979). Magnitude corrections for attenuation in the upper mantle, Geophys. J., 57, 609-638.

McLaughlin, K. L., L. R. Johnson and T. V. McEvilly (1983). Two - dimensional array measurements of near-source ground accelerations, Bull. Seism. Soc. Am., 73, 349-375.

Nuttli, O. W. (1983). A methodology for obtaining seismic yield estimates of underground explosions using short-period Lg waves, in Attenuation of Seismic Waves at Regional Distances, Semi-annual Report (31 March 1983), Saint Louis University, St. Louis, Missouri.

Richards, P. G. and W. Menke (1983). The apparent attenuation of a scattering medium, Bull. Seism. Soc. Am., 73, 1005-1021.

Shumway, R. H. and R. R. Blandford (1978). On detecting and estimating multiple arrivals from underground nuclear explosions, SDAC-TR-77-8, Teledyne Geotech, Alexandria, Virginia.

Stewart, R. R., M. N. Toksoz and A. Timur (1983). Strain dependent attenuation: observations and a proposed mechanism, J. Geophys. Res., 88, 546-554.

von Seggern, D. H. and R. R. Blandford (1972). Source time functions and spectra for underground nuclear explosions, Geophys. J., 31, 83-97.

von Seggern, D. H. and S. S. Alexander (1984). Investigation of source, path and receiver effects for Lg waves from Nevada Test Site explosions, Bull. Seism. Soc. Am. (in press).

DISTRIBUTION LIST
(UNCLASSIFIED REPORTS)
DARPA FUNDED PROJECTS
(Last Revised 19 Nov 1984)

RECIPIENT	NUMBER OF COPIES
DEPARTMENT OF DEFENSE	
DARPA/GSD 1400 Wilson Boulevard Arlington, VA 22209	2
DARPA/PM 1400 Wilson Boulevard Arlington, VA 22209	1
Defense Technical Information Center Cameron Station Alexandria, VA 22314	2
Defense Intelligence Agency Directorate for Scientific and Technical Intelligence Washington, D.C. 20301	1
Defense Nuclear Agency Shock Physics Directorate/SS Washington, D.C. 20305	1
Defense Nuclear Agency/SPSS ATTN: Dr. Michael Shore 6801 Telegraph Road Alexandria, VA 22310	1
DEPARTMENT OF THE AIR FORCE	
AFGL/LW ATTN: Dr. J. Cipar Terrestrial Sciences Division Hanscom AFB, MA 01730	1
AFOSR/NPG ATTN: Director Bldg 410, Room C222 Bolling AFB, Washington D.C. 20332	1
AFTAC/TG Patrick AFB, FL 32925	3
AFTAC/TD (STINFO) Patrick AFB, FL 32925	1
AFWL/NTESC Kirtland AFB, NM 87171	1

DEPARTMENT OF THE ARMY

US Army Engineers 1
ATTN: Mr. J. Drake
Waterways Experiment Station
P.O. Box 631
Vicksburg, MS 39181

DEPARTMENT OF THE NAVY

NORDA 1
ATTN: Dr. J. A. Ballard
Code 543
NSTL Station, MS 39529

DEPARTMENT OF ENERGY

Department of Energy 1
ATTN: Dr. F. Dickerson (DP-52)
International Security Affairs
1000 Independence Avenue
Washington, D.C. 20545

Lawrence Livermore National Laboratory 2
ATTN: Dr. J. Hannon and Dr. M. Nordyke
University of California
P.O. Box 808
Livermore, CA 94550

Los Alamos Scientific Laboratory 1
ATTN: Dr. K. Olsen
P.O. Box 1663
Los Alamos, NM 87544

Sandia Laboratories 1
ATTN: Mr. P. Stokes
Geosciences Department 1255
Albuquerque, NM 87115

OTHER GOVERNMENT AGENCIES

Central Intelligence Agency 1
ATTN: Dr. L. Turnbull
OSI/NED, Room 5G48
Washington, D.C. 20505

U.S. Arms Control and Disarmament Agency 2
ATTN: Mrs. M. Hoinkes
Division of Multilateral Affairs
Washington, D.C. 20301

U.S. Geological Survey 1
ATTN: Dr. T. Hanks
National Earthquake Research Center
345 Middlefield Road
Menlo Park, CA 94025

U.S. Geological Survey 1
ATTN: Dr. Robert Masse
Global Seismology Branch
Box 25046, Stop 967
Denver Federal Center
Denver, CO 80225

UNIVERSITIES

University of California, Berkeley 1
ATTN: DR. T. McEvilly
Department of Geology and Geophysics
Berkeley, CA 94720

California Institute of Technology 1
ATTN: Dr. D. Harkrider
Seismological Laboratory
Pasadena, CA 91125

University of California, San Diego 1
ATTN: Dr. J. Orcutt
Scripps Institute of Oceanography
La Jolla, CA 92093

Columbia University 1
ATTN: Dr. L. Sykes
Lamont-Doherty Geological Observatory
Palisades, NY 10964

Massachusetts Institute of Technology 3
ATTN: Dr. S. Soloman, Dr. N. Toksoz, Dr. T. Jordan
Department of Earth and Planetary Sciences
Cambridge, MA 02139

University of Nevada, Reno 1
ATTN: Dr. A. Ryall
Seismological Laboratory
Reno, NV 89557

The Pennsylvania State University 1
ATTN: Dr. S. Alexander
Department of Mineral Sciences
University Park, PN 16802

Southern Methodist University 1
ATTN: Dr. E. Herrin
Geophysical Laboratory
Dallas, TX 75275

CIRES 1
ATTN: Dr. C. Archambeau
University of Colorado
Boulder, CO 80309

Georgia Institute of Technology 1
ATTN: Professor Anton Dainty
The School of Geophysical Sciences
Atlanta, GA 30332

St. Louis University 1
ATTN: Dr. O. Nuttli
Department of Earth and Atmospheric Sciences
3507 Laclede
St. Louis, MO 63156

DEPARTMENT OF DEFENSE CONTRACTORS

Applied Research Associates, Incorporated 1
ATTN: Dr. N. Higgins
2101 San Pedro Boulevard North East
Suite A
Albuquerque, NM 87110

Applied Theory, Incorporated 1
ATTN: Dr. J. Trulio
930 South La Brea Avenue
Suite 2
Los Angeles, CA 90036

Center for Seismic Studies 2
ATTN: Dr. Carl Romney, and Dr. William Dean
1300 N. 17th Street, Suite 1450
Arlington, VA 22209

ENSCO, Incorporated 1
ATTN: Mr. G. Young
5400 Port Royal Road
Springfield, VA 22151

ENSCO, Incorporated 1
ATTN: Dr. R. Kemerait
1930 Highway A1A
Indian Harbour Beach, FL 32937

Pacific Sierra Research Corporation 1
ATTN: Mr. F. Thomas
12340 Santa Monica Boulevard
Los Angeles, CA 90025

Physics Applications, Incorporated 1
ATTN: Mr. C. Vincent
2340 Harris Way
San Jose, CA 95131

R&D Associates 1
ATTN: Dr. E. Martinelli
P.O. Box 9695
Marina del Rey, CA 90291

Rockwell International 1
ATTN: Dr. B. Tittmann
109 Camino Dos Rios
Thousand Oaks, CA 91360

Gould Incorporated 1
ATTN: Mr. R. J. Woodard
Chesapeake Instrument Division
6711 Baymeado Drive
Glen Burnie, MD 21061

Rondout Associates, Incorporated 1
ATTN: Dr. P. Pomeroy
P.O. Box 224
Stone Ridge, NY 12484

Science Applications, Incorporated 1
ATTN: Dr. T. Bache
P.O. Box 2351
La Jolla, CA 92038

Science Horizons
ATTN: Dr. T. Cherry and Dr. J. Minster 2
710 Encinitas Blvd
Suite 101
Encinitas, CA 92024

Sierra Geophysics, Incorporated 2
ATTN: Dr. R. Hart and Dr. G. Mellman
15446 Bell-Red Road
Redmond, WA 98052

SRI International 1
333 Ravensworth Avenue
Menlo Park, CA 94025

S-Cubed, A Division of
Maxwell Laboratories Inc.
Attn: Dr. Steven Day
P.O. Box 1620
La Jolla, CA 92038 — 1

Maxwell Laboratories Inc
S-Cubed Washington Research Center
Attn: Mr. J. Murphy
11800 Sunrise Valley Drive
Suite 1112
Reston, VA 22091 — 1

Teledyne Geotech
ATTN: Dr. Z. Der & Mr. W. Rivers
314 Montgomery Street
Alexandria, VA 22314 — 2

Woodard-Clyde Consultants
ATTN: Dr. Larry Burdick
556 El Dorado St
Pasadena, CA 91105 — 1

Weidlinger Associates
ATTN: Dr. J. Isenberg
3000 Sand Hill Road
Menlo Park, CA 94025 — 1

NON-U.S. RECIPIENTS

National Defense Research Institute
ATTN: Dr. Ola Dahlman
Stockholm 80, Sweden — 1

Blacknest Seismological Center
ATTN: Mr. Peter Marshall
Atomic Weapons Research Establishment
UK Ministry of Defense
Brimpton, Reading RG7-4RS
United Kingdom — 1

NTNF NORSAR
ATTN: Dr. Frode Ringdal
P.O. Box 51
N-2007 Kjeller
Norway — 1

END

FILMED

1-85

DTIC